

Determination of the top-quark pole mass using $t\bar{t} + 1$ -jet events collected with the ATLAS experiment in 7 TeV pp collisions



The ATLAS collaboration

E-mail: atlas.publications@cern.ch

ABSTRACT: The normalized differential cross section for top-quark pair production in association with at least one jet is studied as a function of the inverse of the invariant mass of the $t\bar{t} + 1$ -jet system. This distribution can be used for a precise determination of the top-quark mass since gluon radiation depends on the mass of the quarks. The experimental analysis is based on proton-proton collision data collected by the ATLAS detector at the LHC with a centre-of-mass energy of 7 TeV corresponding to an integrated luminosity of 4.6 fb^{-1} . The selected events were identified using the lepton+jets top-quark-pair decay channel, where lepton refers to either an electron or a muon. The observed distribution is compared to a theoretical prediction at next-to-leading-order accuracy in quantum chromodynamics using the pole-mass scheme. With this method, the measured value of the top-quark pole mass, m_t^{pole} , is:

$$m_t^{\text{pole}} = 173.7 \pm 1.5 \text{ (stat.)} \pm 1.4 \text{ (syst.)} {}^{+1.0}_{-0.5} \text{ (theory) GeV.}$$

This result represents the most precise measurement of the top-quark pole mass to date.

KEYWORDS: Hadron-Hadron Scattering, Top physics

ARXIV EPRINT: [1507.01769](https://arxiv.org/abs/1507.01769)

Contents

1	Introduction	1
2	Definition of the observable	3
3	The ATLAS experiment	4
4	Data sample and Monte Carlo simulation	4
5	Object definition and basic selection	5
6	Reconstruction of the $t\bar{t} + 1$-jet system	6
7	Top-quark mass determination	8
8	Statistical and systematic uncertainties	14
8.1	Theoretical uncertainties	14
8.2	Detector modelling	15
8.3	Signal modelling	16
8.4	Background modelling	17
8.5	Studies on the definition of the extra jet	18
8.6	Uncertainties on the measured \mathcal{R} -distribution	19
9	Results and discussion	19
	The ATLAS collaboration	25

1 Introduction

In the Standard Model (SM) of particle physics the couplings of the top quark to other particles are fixed through the gauge structure. The only free parameters in the top-quark sector of the SM are the elements of the Cabibbo-Kobayashi-Maskawa mixing matrix and the top-quark mass. Due to its high value compared to the other quark masses, accurate knowledge of the top-quark mass is particularly relevant because it is related to the Higgs-boson and W -boson masses through radiative and loop corrections. The precise determination of these quantities allows a stringent test of whether the model is consistent [1, 2]. In addition, the precise knowledge of the top-quark mass is a crucial ingredient in recent evaluations of the stability of the electroweak vacuum [3–5].

The top-quark mass was determined directly at the Tevatron and at the Large Hadron Collider (LHC). A combination of a subset of these measurements yields a value of $m_t = 173.34 \pm 0.76$ GeV [6]. In these measurements, the top-quark mass is inferred from a

kinematic reconstruction of the invariant mass of its decay products which is then calibrated to the mass definition used in the Monte Carlo (MC) simulations. These m_t determinations lack a clear interpretation in terms of a well-defined top-quark mass theoretical scheme as employed in quantum chromodynamics (QCD) perturbative calculations, electroweak fits or any theoretical prediction in general [2, 6–9]. The values extracted using these methods are usually identified with the top-quark pole mass m_t^{pole} , but present studies estimate differences between the two top-quark mass definitions of $O(1)$ GeV [2, 6–9].

The top-quark mass can also be measured from the inclusive cross section for top-quark pair ($t\bar{t}$) production [10]. With this method the top-quark mass scheme is unambiguously defined in the theoretical calculations. However, top-quark mass determinations based on cross-section measurements are less precise, in their current form, than the other techniques based on kinematic reconstruction. This is due to a relatively weak sensitivity of the inclusive top-quark pair production cross section to the top-quark mass, as well as to the large uncertainties on the factorization and renormalization scales and the proton parton distribution function (PDF). To date, the most precise measurement of this type is based on the 7 TeV and 8 TeV data samples collected by the ATLAS experiment during the years 2011 and 2012, which yields $m_t^{\text{pole}} = 172.9_{-2.6}^{+2.5}$ GeV [11]. The results from the CMS experiment using this technique only include data collected during 2011 [12].

In this paper the method described in ref. [13] is followed. The top-quark mass is extracted from a measurement of the normalized differential cross section $\mathcal{R}(m_t^{\text{pole}}, \rho_s)$ for $t\bar{t}$ production with at least one additional jet, $t\bar{t} + 1\text{-jet}$, as a function of the inverse of the invariant mass of the $t\bar{t} + 1\text{-jet}$ system, $\rho_s \propto 1/\sqrt{s_{t\bar{t}+1\text{-jet}}}$. This distribution is sensitive to the top-quark mass because the amount of gluon radiation depends on its value, with large effects in the phase-space region relatively close to the $t\bar{t} + 1\text{-jet}$ production threshold. This method combines the rigorous interpretation of the mass inferred from the inclusive cross section with the advantage of a greater sensitivity.

The measurement is performed using 7 TeV proton-proton (pp) collision data collected by the ATLAS experiment [14], corresponding to an integrated luminosity of 4.6 fb^{-1} with a total uncertainty of $\pm 1.8\%$ [15]. Events are selected by using the “lepton+jets” final state to identify the $t\bar{t}$ system and at least one additional jet. In this channel one W from the top decay produces a lepton (electron or muon) and a neutrino whereas the other W produces a pair of light quarks. Events are thus required to have exactly one lepton, two jets identified as b -quark jets, at least three additional jets not identified as b -quark jets and a significant amount of missing transverse momentum ($E_{\text{T}}^{\text{miss}}$) due to the neutrino that escapes detection. The differential cross section is corrected to the parton level (a procedure referred to as unfolding in the following) and normalized. The top-quark pole mass is then extracted through a fit to the data using the predicted normalized differential $t\bar{t} + 1\text{-jet}$ cross section from a next-to-leading-order calculation combined with parton showering (NLO+PS) [13, 16–18].

2 Definition of the observable

The method to extract the top-quark pole mass followed here, proposed in ref. [13], exploits the fact that the top-quark mass dependence of the $t\bar{t} + 1$ -jet cross section, $\sigma_{t\bar{t}+1\text{-jet}}$, is enhanced in the phase-space region relatively close to the $t\bar{t} + 1$ -jet production threshold. This method uses the predictions for $t\bar{t} + 1$ -jet production at hadron colliders at NLO accuracy reported in refs. [16, 17]. A well-defined top-quark pole mass can be extracted by comparing these calculations with the measurement of the normalized $t\bar{t} + 1$ -jet cross section in pp collisions as a function of the inverse of the invariant mass $\sqrt{s_{t\bar{t}+1\text{-jet}}}$ of the $t\bar{t} + 1$ -jet system:

$$\mathcal{R}(m_t^{\text{pole}}, \rho_s) = \frac{1}{\sigma_{t\bar{t}+1\text{-jet}}} \frac{d\sigma_{t\bar{t}+1\text{-jet}}}{d\rho_s}(m_t^{\text{pole}}, \rho_s), \quad (2.1)$$

where ρ_s is defined as

$$\rho_s = \frac{2m_0}{\sqrt{s_{t\bar{t}+1\text{-jet}}}}, \quad (2.2)$$

and m_0 is an arbitrary constant of the order of the top-quark mass. Here and in the following, $m_0 = 170$ GeV is used. The anti- k_t jet reconstruction algorithm [19, 20] is employed to reconstruct the jets. The extra jet, beyond those which originated from the $t\bar{t}$ decay, is the leading jet with a transverse momentum $p_T > 50$ GeV and a pseudorapidity $|\eta| < 2.5$.¹ The observable \mathcal{R} defined in this way is infra-red safe as demonstrated in the study of ref. [13].

In this analysis, the measured normalized and differential cross section, unfolded to parton level, is compared to the theoretical calculations at NLO accuracy, after adding the parton shower evolution (NLO+PS). Including the parton shower is expected to give a better description of the final-state phase space than the NLO calculation alone and is implemented in the publicly available MC generator developed in ref. [18]. This generator uses POWHEG (POWHEG-ttJ) [18, 21, 22] matched with the PYTHIA v8 [23] parton shower. Using a fixed order NLO calculation to fit the data gives a similar \mathcal{R} -distribution but leads to an estimated top quark pole mass about 0.3 GeV lower than using a NLO+PS calculation.

This difference is well below the present theoretical uncertainty of the calculation. Differences due to the use of PYTHIA v8 or PYTHIA v6 [24] are below this value of 0.3 GeV.

In the NLO calculation, it is assumed that the top quarks are stable. Possible effects due to radiation from top-quark decay products and virtual corrections to the decay are small compared to the overall theoretical uncertainty. Quantum chromodynamics corrections to the decay do not affect the mass renormalization of the top quark at the same order of accuracy as considered in the calculation because the renormalization is purely determined from the QCD self-energy corrections of the top-quark propagator, which is included in the calculation. Furthermore, recent calculations in refs. [25, 26] include NLO QCD corrections to the total and differential $t\bar{t}$ cross section assuming the top quarks to

¹ATLAS uses a right-handed coordinate system with its origin at the nominal interaction point (IP) in the centre of the detector and the z -axis along the beam pipe. The x -axis points from the IP to the centre of the LHC ring, and the y -axis points upward. Cylindrical coordinates (r, ϕ) are used in the transverse plane, ϕ being the azimuthal angle around the beam pipe. The pseudorapidity is defined in terms of the polar angle θ as $\eta = -\ln[\tan(\theta/2)]$. Transverse momentum and energy are defined as $p_T = p \sin \theta$ and $E_T = E \sin \theta$, respectively.

be off-shell. In this framework, the results in the on-shell approximation are reliable and off-shell effects are at the sub-percent level. In the following, it is assumed that similar results hold for the quantity \mathcal{R} . In fact, as \mathcal{R} is expressed as a normalized cross section, even smaller effects can be expected due to possible cancellations.

3 The ATLAS experiment

The ATLAS experiment [14] is a multipurpose detector with a forward-backward symmetric cylindrical geometry. The inner tracking detector (ID) consists of a silicon pixel detector, a silicon microstrip detector (SCT), and a straw-tube transition radiation tracker (TRT). The ID is surrounded by a thin superconducting solenoid which provides a 2 T magnetic field and by a high-granularity liquid-argon (LAr) sampling electromagnetic calorimeter. The electromagnetic calorimeter is divided into a central barrel ($|\eta| < 1.475$) and end-cap regions at each end of the barrel ($1.375 < |\eta| < 2.5$ for the outer wheel and $2.5 < |\eta| < 3.2$ for the inner wheel). A steel/scintillator-tile calorimeter completes the measurement of hadronic showers in the central pseudorapidity range ($|\eta| < 1.7$), while a LAr hadronic end-cap calorimeter provides coverage over $1.5 < |\eta| < 3.2$. The forward regions ($3.2 < |\eta| < 4.9$) are instrumented with LAr calorimeters for electromagnetic and hadronic measurements. The muon spectrometer (MS) surrounds the calorimeters and consists of three large air-core superconducting toroid systems providing bending powers of 3 Tm in the barrel and 6 Tm in the end-caps, a system of precision tracking chambers ($|\eta| < 2.7$), and fast detectors for triggering ($|\eta| < 2.4$). The combination of all these sub-detectors provides charged-particle measurements together with efficient and precise identification of leptons and photons in the pseudorapidity range of $|\eta| < 2.5$. Jets and $E_{\text{T}}^{\text{miss}}$ are reconstructed using energy deposits over the full coverage of the calorimeters, $|\eta| < 4.9$. The reconstructed muon momenta are also included in the evaluation of $E_{\text{T}}^{\text{miss}}$. Evaluation of the luminosity scale is performed using several luminosity-sensitive detectors. The ATLAS experiment has a three-level trigger system [14]. The first-level trigger is hardware-based and uses a subset of the detector information to reduce the event rate to at most 75 kHz. The second and third levels are software-based and together reduce the event rate to about 300 Hz.

4 Data sample and Monte Carlo simulation

The data considered in this analysis correspond to an integrated luminosity of 4.6 fb^{-1} of proton-proton collisions at a centre-of-mass energy of 7 TeV. They were recorded in 2011 during periods with stable beam conditions and with all relevant subdetector systems operational. The events were selected by single-lepton triggers that require a minimum transverse momentum of 18 GeV for muons and a minimum of 20 to 22 GeV for electrons, depending on the data-taking conditions.

In this analysis, several MC samples are used for the modelling of $t\bar{t}$ pair production and the main background processes. For the simulation of the $t\bar{t}$ signal and the unfolding, the POWHEG code (POWHEG-hvq, *patch4* [27]) is used to calculate the QCD matrix element at NLO with the CT10 [28] PDF set. The parton shower and the underlying event

are added using the PYTHIA v6.4 [24] generator with the Perugia 2011C parameter set (tune) [29]. Several MC sets of events were generated using different top-quark masses. The nominal MC sample, which is used in the present study to compare the MC predictions with data, is the largest and is produced assuming a top-quark mass of $m_t = 172.5$ GeV. The corresponding cross section of the nominal $t\bar{t}$ sample is 177_{-11}^{+10} (theo.) pb as predicted by the calculations in refs. [30–34], which include the next-to-next-to-leading order (NNLO) and the resummation of next-to-next-to-leading logarithmic (NNLL) soft gluon terms with $\text{top}++2.0$ [33]. In addition to this nominal sample, five other samples are employed with different assumptions about the input top-quark mass in the range from 167.5 GeV to 180 GeV in steps of 2.5 GeV.

Background processes to the $t\bar{t} + 1\text{-jet}$ final state under study are simulated with various MC generators. Single top quark production in the s -, Wt - and t -channels is simulated using POWHEG matched with PYTHIA v6.4. The Perugia 2011C tune is used. The production of W/Z bosons in association with jets (W +jets or Z +jets) is simulated using the ALPGEN generator (v2.13) [35] with the leading-order (LO) CTEQ6L1 [36] PDF set. These calculations are interfaced with HERWIG 6 [37] for the parton shower and JIMMY v4.31 [38] for the underlying-event modelling. W +jets events containing heavy-flavour quarks are generated separately using leading-order matrix elements with massive b - and c -quarks. Possible double-counting due to heavy quarks produced by the parton shower is considered and removed. The total number of W +jets events is normalized by exploiting the lepton charge asymmetry observed in data, following the method in ref. [39]. Diboson events (WW , ZZ , WZ) are generated using HERWIG 6 with the MRSTMCal [40] PDF. The background from misidentified and non-prompt leptons is estimated using a data-driven matrix method described in ref. [41].

Multiple soft pp interactions generated with PYTHIA v6.425 using the AMBT2B tune [42] are added to all simulated events in order to account for the effect of multiple pp interactions in the same and neighbouring bunch crossings (pile-up).

The response of the ATLAS detector is simulated using a detailed description of the detector geometry [43] in GEANT4 [44]. Simulated events are reconstructed using the same software as used for the data.

5 Object definition and basic selection

The analysis applies several requirements to the events and makes use of reconstructed electrons, muons, jets and E_T^{miss} . Electron candidates are reconstructed from energy deposits in the electromagnetic calorimeter using criteria based on the shower shape, and they must be matched to a charged-particle track in the ID [45]. Electrons must have a transverse momentum of $p_T > 25$ GeV and $|\eta| < 2.47$. Events with electrons falling in the calorimeter barrel/end-cap transition region, corresponding to $1.37 < |\eta| < 1.52$, are rejected. Muon candidates are identified by combining track candidates in the MS and the ID [46]. All muons are required to have a transverse momentum $p_T > 25$ GeV and $|\eta| < 2.5$. All muons must additionally satisfy a series of selection criteria on the number

of hits per track in the various tracking sub-detectors [47]. Finally, electrons and muons have to match corresponding objects that have fired the trigger.

Isolation criteria are applied to electron and muon candidates to reduce the background from hadrons mimicking lepton signatures and backgrounds from heavy-flavour decays inside jets [48].

Energy deposits in the calorimeters are combined into three-dimensional clusters [49]. From these clusters, jets are reconstructed using the anti- k_t jet algorithm with a radius parameter of 0.4. Reconstructed jet energies in simulations are calibrated from stable-particle jets. Residual calibrations, derived by using in situ methods where the jet transverse momentum is compared to that of a reference object (e.g. using γ/Z +jet events), are then applied to data relative to the simulations [50].

Reconstructed jets must have $p_T > 25$ GeV and $|\eta| < 2.5$. To suppress the contribution from low- p_T jets originating from pile-up interactions, a jet vertex fraction requirement is applied: at least 75% of the summed scalar p_T of tracks associated with the jet must be due to tracks originating at the event primary vertex. This primary vertex is defined as the vertex with the highest $\sum_{\text{trk}} (p_T^{\text{trk}})^2$ among all candidates with at least five associated tracks (trk) with $p_T^{\text{trk}} > 0.4$ GeV [51]. Jets containing b -hadrons are identified using a neural network exploiting the long lifetime of b -hadrons at a working point resulting in a tagging efficiency of 70% in simulated $t\bar{t}$ events [52–54].

The transverse momentum of neutrinos escaping the detector is assumed to be identical to E_T^{miss} , which is reconstructed as the magnitude of the momentum imbalance in the transverse plane as obtained from the negative vector sum of the momenta of all energy deposits. It is reconstructed from topological clusters, calibrated for electromagnetic objects and corrected according to the energy scale of the identified objects. Muons contributions are also included by using their momentum measured in the inner detector and the muon spectrometer [55].

Events must not contain jets with p_T greater than 20 GeV arising from out-of-time energy deposits or from energy deposits with a hardware or calibration problem. Exactly one isolated electron or muon, and at least five jets are required with exactly two of the jets tagged as b -quark jets. The magnitude of the missing transverse momentum and the transverse mass of the system formed by the charged lepton and the neutrino,² m_T^W , must both exceed 30 GeV.

6 Reconstruction of the $t\bar{t} + 1$ -jet system

After the basic selection, a kinematic reconstruction of the events is performed to identify the W -boson and top-quark candidates. The leptonically-decaying W boson is identified with the charged lepton and the neutrino, where the longitudinal momentum is inferred using a constraint on the W -boson mass. Candidates for the hadronically-decaying W boson are constructed by considering all possible pairs of jets among those not identified

²The W -boson transverse mass is defined as $m_T^W = \sqrt{2p_{T,\ell} p_{T,\nu} [1 - \cos(\phi_\ell - \phi_\nu)]}$ where ℓ and ν refer to the selected lepton and the neutrino whose information is associated with the E_T^{miss} vector, respectively.

	Events	Uncertainty
Signal ($t\bar{t}$, $m_t = 172.5$ GeV)	2050	± 320
W +jets	31	± 16
Z +jets	6	± 4
Single top ($m_t = 172.5$ GeV)	62	± 34
WW, ZZ, WZ	1	± 1
Misidentified and non-prompt leptons	22	± 13
Total Background	121	± 40
Total Predicted	2170	± 320
Data	2256	

Table 1. Event yields and their uncertainties after the reconstruction of the $t\bar{t} + 1$ -jet system. The quoted uncertainty values include the total statistical and systematic uncertainties as described in section 8.

as b -jets. Accepted events must fulfil the following conditions:

$$0.9 < \alpha \equiv \frac{m_W^{\text{ref}}}{m_{ij}} < 1.25, \tag{6.1}$$

$$\Delta k_t(i, j) \equiv \min(p_T^i, p_T^j) \cdot \Delta R(i, j) < 90 \text{ GeV}, \tag{6.2}$$

where the indices i and j run over all jets not identified as b -jets, m_{ij} is the invariant mass of jets i and j , and $m_W^{\text{ref}} = 80.4$ GeV [56]. All combinations of the two b -jets with the W -boson candidates are considered as top-quark candidates. Once both requirements are applied, the permutation that minimizes the invariant mass difference of the hadronically and leptonically decaying top-quark candidates is selected. The application of these two requirements reduces the combinatorial background.

The magnitude of the momentum vectors of the light-quark jets associated with the hadronic W boson are scaled using the value of α derived from eq. (6.1). A further requirement on the ratio of the reconstructed top-quark kinematic mass for the leptonic and hadronic decays, $m_t^{\text{leptonic}}/m_t^{\text{hadronic}} > 0.9$, is imposed to increase the signal to background ratio. The leading- p_T jet is selected among the remaining jets and is identified as the extra jet completing the $t\bar{t} + 1$ -jet system. The extra jet must satisfy $p_T > 50$ GeV and $|\eta| < 2.5$.

The event yields after the final selection are presented in table 1. The number of selected data events is in good agreement with the MC expectation.

After applying all the selection criteria, data were compared to the expectations. A representative subset of kinematic and angular distributions is shown in figures 1 and 2. In all cases, good agreement between data and prediction is observed. In addition to these plots, the number of reconstructed $t\bar{t} + 1$ -jet events as a function of ρ_s is shown in figure 3.

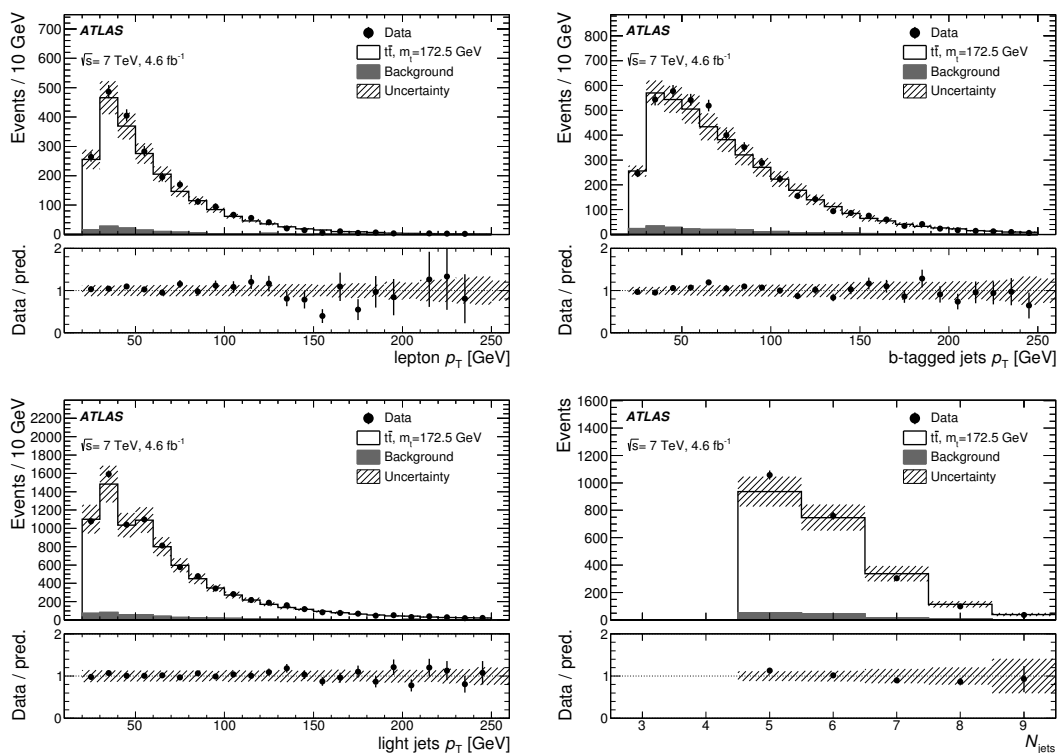


Figure 1. The data for various kinematic distributions (transverse momentum, p_T , of the lepton, p_T of all the b -tagged jets, p_T of all non- b -tagged jets and the total jet multiplicity) are compared to the nominal $t\bar{t}$ MC sample (POWHEG+PYTHIA) plus backgrounds after the final kinematic reconstruction of the $t\bar{t}+1$ -jet events. The total background estimated in table 1 is shown in dark grey. The uncertainty band includes the total statistical and systematic uncertainties as described in section 8.

7 Top-quark mass determination

The top-quark pole mass is extracted by fitting the parameterized NLO+PS prediction to the measured distribution of the normalized differential cross section \mathcal{R} defined in eq. (2.1) after background subtraction and correction for detector effects and hadronization. This method follows a similar procedure to that employed in ref. [57]. The observed number of $t\bar{t}+1$ -jet events in figure 3 is used to construct this \mathcal{R} -distribution at parton level.

The recorded parton-level information in the nominal ATLAS signal MC sample (see section 4) did not allow the construction of the extra jet at the parton level, as required by the theoretical calculation. Consequently, a simple direct connection between the $t\bar{t}+1$ -jet system at detector level and at parton level could not be made. For that reason, an intermediate state corresponding to the first gluon emission at parton level ($t\bar{t}+g$) was introduced to bridge the connection and an additional MC sample of events was generated. This latter sample transformed the \mathcal{R} -distribution of the $t\bar{t}+g$ system into the final \mathcal{R} -distribution of the $t\bar{t}+1$ -jet system, which this time was defined as in the theoretical

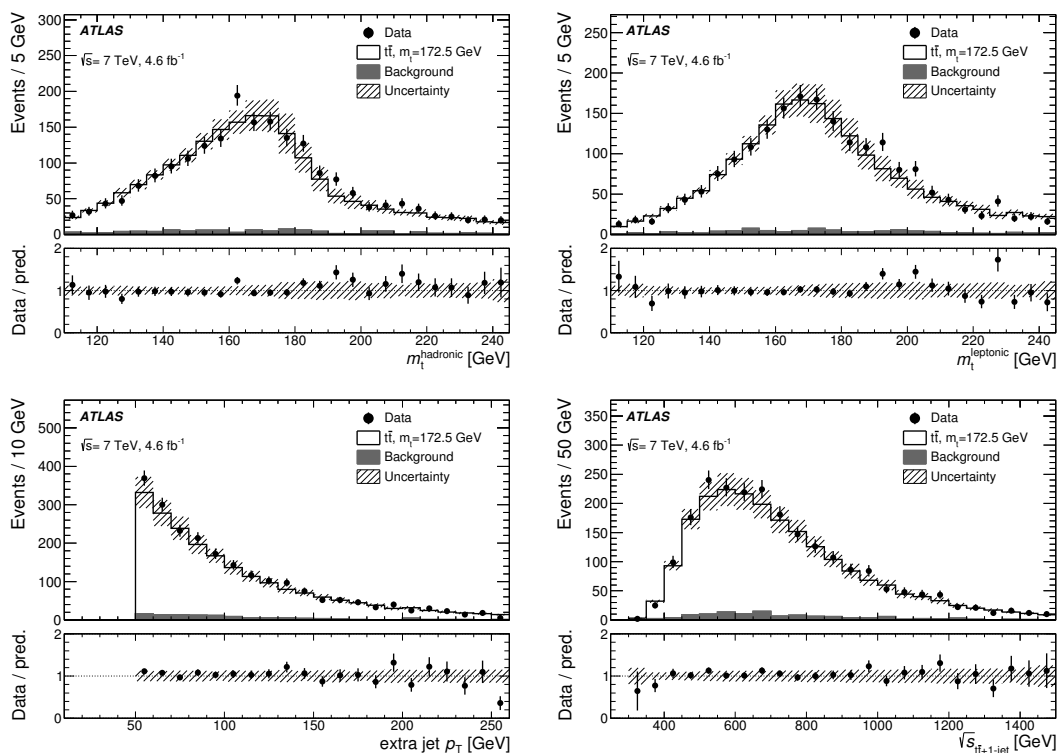


Figure 2. The data for various kinematic distributions (the reconstructed mass of the hadronically and leptonically decaying top-quark candidates, the p_T of the additional jet and the invariant mass of the $t\bar{t} + 1$ -jet system) are compared to the nominal $t\bar{t}$ MC sample (POWHEG+PYTHIA) plus backgrounds after the final kinematic reconstruction of the $t\bar{t} + 1$ -jet events. The total background estimated in table 1 is shown in dark grey. The uncertainty band includes the total statistical and systematic uncertainties as described in section 8.

calculation. This sample was validated using ATLAS procedures and did not include the full detector simulation. The final correction procedure contained the following steps:

$$t\bar{t} + 1\text{-jet (detector level)} \rightarrow t\bar{t} + g \text{ (parton level)} \rightarrow t\bar{t} + 1\text{-jet (parton level)},$$

As a first step the migration matrix relating the distribution of $t\bar{t} + 1$ -jet events at detector level and the $t\bar{t} + g$ events at parton level was calculated using the nominal MC simulation. Data were grouped in bins as a function of ρ_s with a variable bin size as displayed in table 2 and in figure 4. This choice was the result of a compromise between having values of the diagonal terms in the migration matrix above 50% and optimizing the sensitivity of the \mathcal{R} -distribution to the top-quark mass according to the study of ref. [13]. The migration matrix was then inverted using the Singular Value Decomposition (SVD) method described in ref. [58]. This algorithm minimizes the statistical fluctuations inherent in the matrix-inversion process.

The above correction restricts the kinematical phase-space region to that of the events satisfying the selection criteria. Hence an additional correction is needed to extend this region to the full acceptance considered by the theoretical calculation (acceptance term).

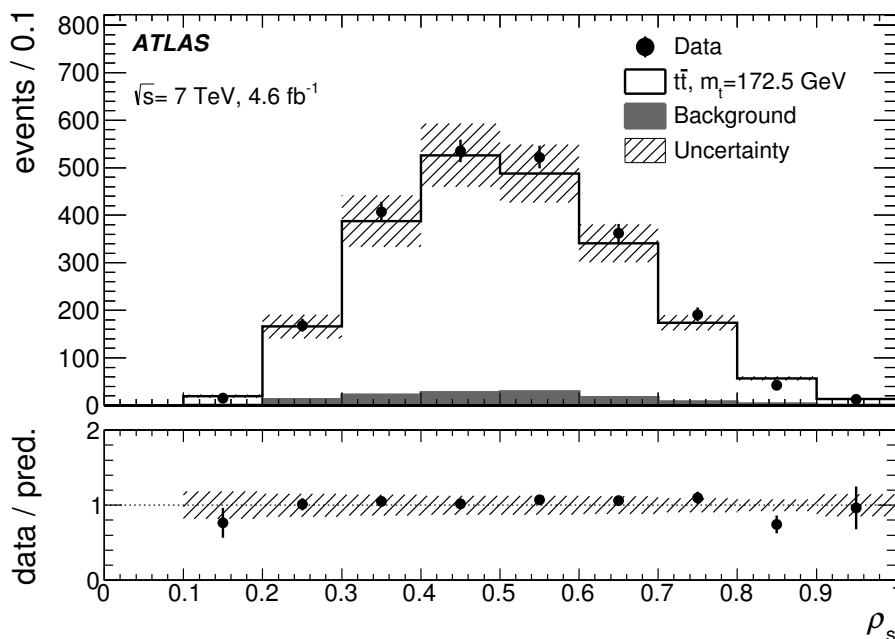


Figure 3. Number of reconstructed events as a function of ρ_s ($m_0 = 170$ GeV) related to the inverse of the invariant mass of the $t\bar{t} + 1$ -jet system. The data are compared to the nominal $t\bar{t}$ MC prediction (POWHEG+PYTHIA) plus backgrounds, which assumes a top-quark mass $m_t = 172.5$ GeV after the final kinematic reconstruction of the $t\bar{t} + 1$ -jet events. The backgrounds and the systematic uncertainties are estimated as in figure 1 and 2.

Finally an additional step was implemented to convert the \mathcal{R} -distribution corresponding to the $t\bar{t}+g$ system into the \mathcal{R} -distribution of the $t\bar{t} + 1$ -jet system defined as in the theoretical calculation. The final unfolding procedure is described as follows:

$$\mathcal{R}^{\text{cor-data}}(\rho_s) \equiv \left[\left(\mathcal{M}^{-1} \otimes \mathcal{R}^{\text{det-data}}(\rho_s) \right) \cdot \left(\frac{\mathcal{R}^{\text{acc.}}(\rho_s)}{\mathcal{R}^{\text{tt+g}}(\rho_s)} \right)^{-1} \right] \cdot \left(\frac{\mathcal{R}^{\text{tt+1-jet}}(\rho_s)}{\mathcal{R}^{\text{tt+g}}(\rho_s)} \right), \quad (7.1)$$

where $(\mathcal{M}^{-1} \otimes \mathcal{R}^{\text{det-data}}(\rho_s))$ is the term describing the transformation of the $t\bar{t} + 1$ -jet distributions from detector level to the parton level at its first gluon emission ($t\bar{t}+g$). The acceptance term is

$$\left(\frac{\mathcal{R}^{\text{acc.}}(\rho_s)}{\mathcal{R}^{\text{tt+g}}(\rho_s)} \right)^{-1}, \quad (7.2)$$

and deviates from unity by less than 2% over the full ρ_s range. The factor

$$\left(\frac{\mathcal{R}^{\text{tt+1-jet}}(\rho_s)}{\mathcal{R}^{\text{tt+g}}(\rho_s)} \right), \quad (7.3)$$

transforms the \mathcal{R} -distribution which corresponds to the $t\bar{t}+g$ system into the \mathcal{R} -distribution of the $t\bar{t} + 1$ -jet system. This correction factor is typically within 10% of unity.

ρ_s ($m_0 = 170$ GeV) \diagdown m_t^{pole}	$\mathcal{R}^{\text{theory}}$				
	170 GeV	172.5 GeV	175 GeV	177.5 GeV	180 GeV
0 to 0.25	0.1327(9)	0.1390(44)	0.1425(8)	0.1487(10)	0.1548(6)
0.25 to 0.325	1.104(14)	1.134(6)	1.172(13)	1.208(15)	1.251(9)
0.325 to 0.425	1.972(9)	2.027(4)	2.070(9)	2.130(11)	2.185(7)
0.425 to 0.525	2.506(12)	2.561(6)	2.587(11)	2.644(13)	2.674(8)
0.525 to 0.675	2.143(8)	2.125(4)	2.116(7)	2.085(9)	2.060(6)
0.675 to 1.0	0.353(2)	0.316(1)	0.287(2)	0.252(2)	0.223(1)

Table 2. The \mathcal{R} -distribution calculated using generated $t\bar{t} + 1$ -jet samples at NLO+PS accuracy for different m_t^{pole} values at parton level (corresponding to $\mathcal{R}^{\text{theory}}$ in eq. (7.5)). The quoted uncertainties in parentheses reflect the statistical precision of the calculation.

In more detail, the first part of eq. (7.1) corresponds to:

$$\left(\mathcal{M}^{-1} \otimes \mathcal{R}^{\text{det-data}}(\rho_s)\right)_i \equiv \frac{1}{N_{\text{tot}}^{t\bar{t}+1\text{-jet}}} \frac{\sum_j M_{ij}^{-1} \cdot N_j^{t\bar{t}+1\text{-jet}}}{\Delta\rho_s^i}, \quad (7.4)$$

where i, j refers to the bin numeration defined for the ρ_s variable, $N_j^{t\bar{t}+1\text{-jet}}$ is the number of $t\bar{t} + 1$ -jet events reconstructed (background subtracted) in the j -th bin, $N_{\text{tot}}^{t\bar{t}+1\text{-jet}}$ is the total number of reconstructed $t\bar{t} + 1$ -jet events (background subtracted), M_{ij}^{-1} is the inverse of the migration matrix and $\Delta\rho_s^i$ is the width of the i -th bin.

Once data were properly corrected, the value of m_t^{pole} was determined by fitting the unfolded \mathcal{R} -distribution with the NLO+PS prediction from ref. [18] using the least-squares method. Table 2 shows the predicted values of \mathcal{R} ($\mathcal{R}^{\text{theory}}$) in bins of ρ_s for different m_t^{pole} values. The fit minimized a χ^2 defined as:

$$\chi^2 = \sum_{ij} (\mathcal{R}_i^{\text{cor-data}} - \mathcal{R}_i^{\text{theory}}(m_t^{\text{pole}})) V_{ij}^{-1} (\mathcal{R}_j^{\text{cor-data}} - \mathcal{R}_j^{\text{theory}}(m_t^{\text{pole}})), \quad (7.5)$$

where $\mathcal{R}_i^{\text{cor-data}}$ is the data value in the i -th bin of the corrected \mathcal{R} -distribution and V^{-1} is the inverse of the statistical covariance matrix of the unfolded \mathcal{R} -distribution. The quantity $\mathcal{R}_i^{\text{theory}}(m_t^{\text{pole}})$ represents the theoretical prediction for the i -th bin and contains the dependence on the top-quark pole mass. The covariance matrix is obtained by producing a sample of 500 pseudo-experiments scattered around the measured values of the \mathcal{R} -distributions assuming Gaussian statistical errors. Each of these pseudo- \mathcal{R} -distributions was then corrected following the unfolding procedure described above and finally the covariance matrix (V) was evaluated accordingly.

The inferred m_t^{pole} value is the one which minimizes the χ^2 in eq. (7.5) calculated by considering all bins except for the least sensitive one ($0 \leq \rho_s < 0.25$). This is done because the \mathcal{R} -distribution is constrained by the normalization condition. The extracted mass value does not significantly depend on this bin choice. The selected configuration is the one which gives the highest expected precision. The statistical uncertainty is taken as

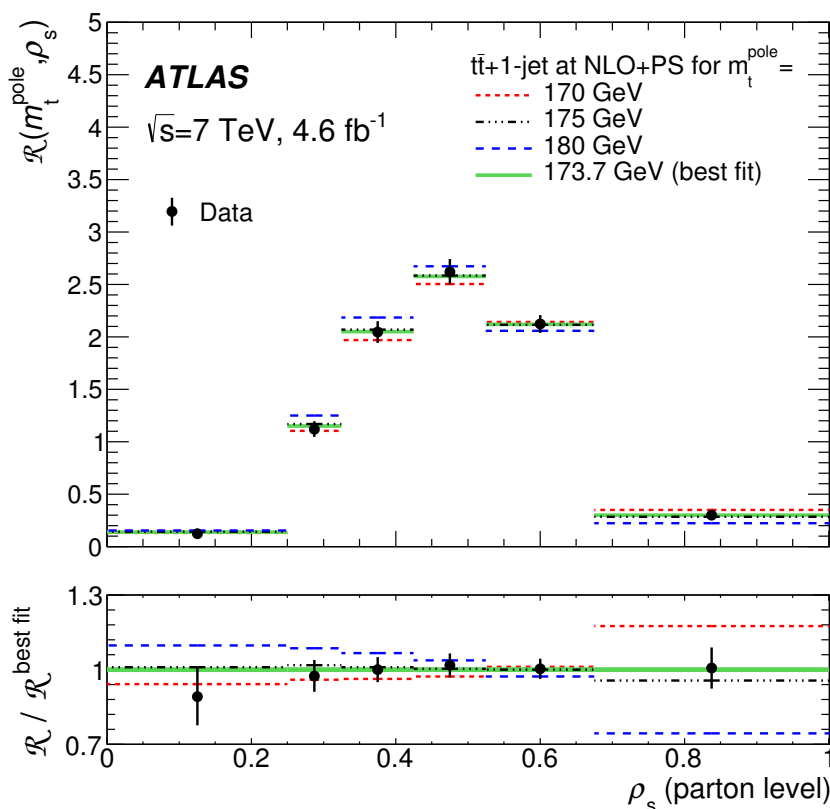


Figure 4. \mathcal{R} -distribution at parton level corrected for detector and hadronization effects after the background subtraction as a function of ρ_s ($m_0 = 170$ GeV). The predictions of the $t\bar{t}+1$ -jet calculation at NLO+PS using three different masses ($m_t^{\text{pole}} = 170, 175$ and 180 GeV) are shown together with the result of the best fit to the data, $m_t^{\text{pole}} = 173.7 \pm 1.5$ (stat.) GeV. The black points correspond to the data. In the lower part of the figure, the ratios of the different \mathcal{R} -distributions to the one corresponding to the best fit are shown. The shaded area indicates the statistical uncertainty.

the mass shift that increases the χ^2 by one unit with respect to the minimum ($\Delta\chi^2 = +1$). The possible impact of non-perturbative effects near the threshold for $t\bar{t}+1$ -jet production ($\rho_s \sim 1$) was also studied by choosing a restricted range of ρ_s from 0 to 0.9 and by studying the results for each bin independently. No significant effect is observed.

The corrected \mathcal{R} -distribution is shown in figure 4. For comparison purposes the predictions for three top-quark pole mass values are also shown ($m_t^{\text{pole}} = 170, 175$ and 180 GeV) together with the top-quark mass extracted from the best fit, which is $m_t^{\text{pole}} = 173.7 \pm 1.5$ (stat.) GeV. Only the statistical uncertainty is shown in this figure.

The corrections for detector and hadronization effects based on the MC simulation might introduce a dependence on the input top-quark mass assumed in the generator. The possible impact was quantified by generating input $t\bar{t}+1$ -jet distributions using fully simulated samples with POWHEG + PYTHIA and with different MC masses ranging from 167.5 GeV to 180 GeV, i.e. keeping the same nominal MC parameter set except for the input top-quark mass. Each of the corresponding distributions is unfolded with the same

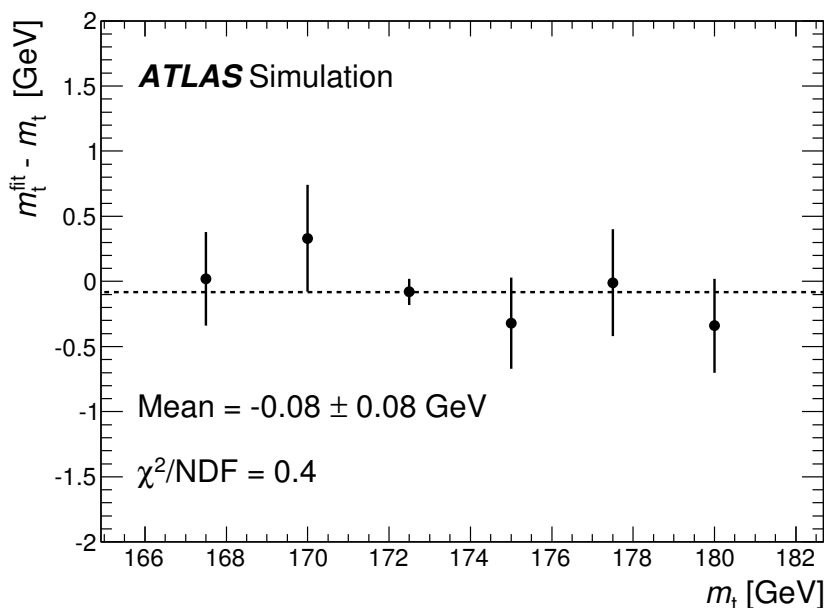


Figure 5. Difference between the fitted mass and the top-quark mass assumed in the generated $t\bar{t}$ MC predictions (POWHEG+PYTHIA) including full detector simulation as a function of the input mass. The same unfolding procedure employed for data is performed in this study. The migration matrix and correction factors are defined for a fixed top-quark mass of $m_t = 172.5$ GeV. The fit is performed using the parameterised mass dependence of the theoretical predictions obtained from the MC samples. A fit to a straight line including the point at 172.5 GeV is performed. The obtained mean value and χ^2/NDF are shown.

procedure as used for data, fixing the migration matrix and correction factors, which are defined for a fixed top-quark mass of $m_t = 172.5$ GeV. Fits to the resulting \mathcal{R} -distributions are performed using the parameterised mass dependence of the theoretical predictions obtained from the MC samples with input top-quark masses between 167.5 GeV and 180 GeV. Each top-quark mass extracted is compared with the corresponding input top-quark mass. Figure 5 shows the difference between the input and fitted masses as a function of the input mass. In the range studied here, all fit results are compatible with the input values within their statistical uncertainties.

Existing generated samples with POWHEG + HERWIG 6 including full ATLAS simulation were used to make the correction of the data without using the intermediate state of the $t\bar{t}+g$ system. This cross-check allowed investigations of potential biases introduced by this step. When using this sample the correction procedure was tested including and excluding the $t\bar{t}+g$ intermediate state. The two methods gave compatible results within ~ 0.1 GeV for m_t^{pole} , well within the statistical precision of the test, ~ 0.25 GeV.

8 Statistical and systematic uncertainties

This section describes the uncertainties that affect the extraction of the top-quark pole mass. The statistical uncertainty of the corrected result is evaluated using eq. (7.5) using toy MC experiments to derive the covariance matrix of the fit. The additional (small) uncertainty due to the limited number of MC events used to define the unfolding procedure is evaluated by varying the migration matrix according to their statistical uncertainties. The systematic uncertainties are split into four categories: theoretical uncertainties, signal- and detector-modelling uncertainties, and finally background uncertainties. They are described in the following subsections and summarized in table 3.

8.1 Theoretical uncertainties

Scale variations: the calculation of \mathcal{R} is performed by setting the renormalization scale (μ_R) equal to the factorization scale (μ_F). To estimate the uncertainty due to the missing higher-order terms in the calculation, these scales are varied around the central values $\mu = \mu_R = \mu_F = m_t^{\text{pole}}$ by a factor of two up and down. The data were fitted using the predictions with a scale μ twice or half the nominal value ($\mu = 2m_t^{\text{pole}}$, $\mu = m_t^{\text{pole}}/2$). The alternative choices for the scale lead to a 0.44 GeV lower value for the top-quark pole mass for $\mu = 2m_t^{\text{pole}}$ and to a 0.93 GeV higher value for $\mu = m_t^{\text{pole}}/2$.

In principle one could also vary the factorization scale independently from the renormalization scale. This exercise was considered in ref. [18] and the results obtained showed very good agreement with those from the restricted scale variation considered in ref. [17]. As a consequence no significant changes in the estimation of this uncertainty are expected when considering an independent variation of the scales.

It is often argued that for normalized cross sections the method described above to evaluate the effect of uncalculated higher order terms in the perturbative calculations might be unrealistic and reduce its dependence due to cancellations of α_s in the ratio. Therefore a different approach to evaluate this uncertainty was considered in ref. [13]. It consisted of expanding the \mathcal{R} -distribution in powers of α_s , thus avoiding the ratio. It was found that the two methods gave consistent estimates of the uncertainty.

In addition to these cross-checks the size of the NLO correction with respect to the LO was also computed for \mathcal{R} . The study compared the LO+PS prediction using a fixed scale $\mu = m_t$ and a variable dynamic scale $\mu = \sqrt{m_t^2 + p_{T,t}^2}$ to the NLO+PS prediction with fixed scale. Differences in the range from 0.6 to 0.8 GeV were observed. The small NLO correction indicates that the calculation converges well.

Proton PDF and α_s : the uncertainties on the proton PDF and on the value of the strong coupling constant α_s used in the $t\bar{t} + 1$ -jet calculation are propagated by fitting to various \mathcal{R} -distributions implemented in NLO+PS calculations using different PDF sets with different α_s values. The central CT10 [59], MSTW2008nlo90cl [60, 61] and NNPDF [62] PDF sets were employed to estimate this uncertainty. For each of these sets the central value of the resulting top-quark mass was calculated and the

uncertainty due to the PDF corresponds to half of the maximum difference. The impact of varying only α_s was estimated and found to be very small, $\sigma\left(m_t^{\text{pole}}\right) = 0.01 \text{ GeV}$ (for $\Delta\alpha_s = \pm 0.002$ and the CT10 PDF set) since the dependence of \mathcal{R} on α_s nearly vanishes due to the use of a normalized differential distribution.

The total theoretical uncertainty is the sum in quadrature of the contributions of scale variations and the PDF and α_s uncertainties.

8.2 Detector modelling

The uncertainties on the reconstruction efficiency and the energy measurement of basic reconstructed objects (leptons, E_T^{miss} and jets) are propagated to the uncertainty on the value of the top-quark mass. Variations of all these quantities by ± 1 standard deviation are implemented in MC samples that are then unfolded using the nominal response matrix. A fit to the resulting \mathcal{R} -distribution is performed and the top-quark mass is extracted. In the following — unless otherwise stated — the systematic uncertainties arising from the different modelling sources are calculated as half of the difference between the upward and downward variations.

Jet energy scale (JES) and b -jet energy scale: to estimate the impact of the jet energy scale uncertainty on the result, the jet energy is scaled up and down by its uncertainty for 21 uncorrelated components which are considered separately [50, 63]. These are the experimental sources of uncertainty with the largest impact on the precision of the mass determination.

Jet energy resolution and jet reconstruction efficiency: the effect of the jet energy resolution uncertainty is evaluated by smearing, before the event selection, the energy of the jets by a Gaussian function with a width chosen in agreement with the jet energy resolution uncertainty. The effect of the jet reconstruction efficiency uncertainty is evaluated by randomly discarding a fraction of jets from the events before the selection [64].

b -tagging efficiency and mistag rate: differences in the b -tagging efficiency as well as c -jet and light-jet mistag rates in data and simulation are parameterized using correction factors, which are functions of p_T and η . These corrections are derived from data including $t\bar{t}$ events and they are varied by their uncertainties (see refs. [52–54]). Similarly to the JES uncertainty, the uncertainty on the correction factors for the b -tagging efficiency is separated into several uncorrelated components. The systematic uncertainty is assessed by changing the correction factor central values by $\pm 1\sigma$ for each component, and performing the mass extraction. The final uncertainty due to the b -tagging efficiency is calculated as the quadratic sum of all contributions.

Lepton identification and lepton energy resolution: the correction factors applied to the lepton identification are measured by comparing high-purity events from simulation and data including Z , W and J/ψ decays for electrons [45], and Z , W , J/ψ and Υ decays for muons [47]. For the measurement of the lepton energy or momentum

scale uncertainties, a similar procedure is used. The systematic uncertainties associated to each correction factor are estimated by changing its central value by $\pm 1\sigma$ and applying the mass extraction procedure. The quadratic sum of all contributions gives the quoted final uncertainty due to this source.

Modelling of the E_T^{miss} : uncertainties on the energy scale of jets or leptons are also propagated to the uncertainty of the E_T^{miss} . Other contributions to this uncertainty originate from the energy scale and resolution of the soft calorimeter energy deposits which are not included in the reconstructed jets and leptons, and contribute only to the estimation of E_T^{miss} . The E_T^{miss} is scaled up and down by its uncertainty. The effect of these changes is propagated to the simulated events allowing to evaluate the impact on the top-quark mass measurement following the same procedure as for the rest of systematic uncertainties.

8.3 Signal modelling

The signal modelling uncertainties originate from: the choice of matrix element, the parton shower and hadronization model, and the choice of the PDF set used in the simulation of $t\bar{t}$ events. In addition, uncertainties on the modelling of the initial- and final-state QCD radiation (ISR/FSR), of colour reconnection, and of the underlying event are also accounted for. Their impact on the extracted mass is estimated using alternative MC samples. The alternative \mathcal{R} -distribution samples are corrected using the nominal response matrix and the deviation from the result of the nominal MC sample is used to estimate the uncertainty.

MC generator and hadronization: the uncertainty associated with the choice of MC generator is evaluated by comparing two NLO MC generators interfaced to the same parton shower and hadronization program: POWHEG-BOX [21, 22] and MC@NLO [65] both interfaced to HERWIG 6 are compared. The difference between the extracted masses is taken as the generator uncertainty.

The uncertainty associated with the hadronization is estimated by comparing the results obtained with POWHEG interfaced to either PYTHIA or HERWIG 6. The full difference is quoted as the hadronization uncertainty.

Initial- and final-state radiation (ISR/FSR): the effect of the ISR and FSR modelling uncertainties is evaluated by comparing two simulated signal samples with varied radiation settings. The samples to evaluate the ISR/FSR uncertainty are generated with ALPGEN(v2.13) [35]+PYTHIA, which is a multileg MC generator that generates, at LO, $t\bar{t}$ plus up to five partons. The samples to estimate the ISR/FSR uncertainty correspond to variations of the $KTFAC$ parameter in ALPGEN between a factor two up and down of its nominal value (with the Perugia 2011 radLow and radHi tunes respectively [29]). This parameter determines the scale at which α_s is evaluated for additional gluon emissions and the size of the variation considered is compatible with the measurements of additional jet activity in $t\bar{t}$ events [66]. The ISR/FSR uncertainty is evaluated by taking half the difference between the fitted top-quark masses from the two samples.

Colour reconnection and underlying event: the impact of the uncertainties in the MC models describing colour reconnection and the underlying event is estimated by comparing several POWHEG MC samples with different tunes. The effect of the colour reconnection modelling uncertainty is estimated as the difference between the result obtained with the nominal POWHEG sample with the Perugia 2012 (P2012) tune and an alternative sample with the Perugia 2012 loCR tune [29]. To estimate the uncertainty on the underlying event modelling, the Perugia 2012 mpiHi tune [67] is compared with the P2012 tune. In both cases the full mass difference from the default value is taken as the systematic uncertainty.

Proton PDF: uncertainties on the proton PDF give rise to uncertainties on the efficiency of the basic event selection. These uncertainties are calculated following the PDF4LHC recommendations [68] using $t\bar{t}$ events simulated by MC@NLO interfaced to HERWIG 6. This uncertainty accounts for the effects of the PDF on the theoretical modelling of the $t\bar{t}$ system, the hadronization and the experimental data analysis. To a large extent the first contribution is already considered in the evaluation of the theoretical uncertainties of section 8.1. In the present work the two uncertainties are considered independently. This evaluation of the total PDF uncertainty is therefore regarded as a conservative approach. Using the values from table 3 and considering both uncertainties either completely correlated or uncorrelated changes the overall uncertainty on the PDF from 0.54 GeV to 0.58 GeV which has a rather minimal impact.

8.4 Background modelling

The uncertainty on the background yield is taken into account by varying the normalization and the shape of the distributions of several contributing processes. For both W +jets and Z +jets production, the uncertainty on the normalization is studied following the recommendations in ref. [69]. For the 5-jet final state, a total uncertainty of 54% is assessed [69]. For the W +jets background, the shape uncertainties due to the events with jets originating from heavy-flavour quarks are studied by varying the fraction of these events in the sample. The evaluation for this analysis follows the method described in ref. [39]. The shape and normalization uncertainties on the misidentified and non-prompt lepton component are propagated to the top-quark mass. The most important background topologies originate from single-top plus jets production. The impact on the top-quark mass is estimated by comparing the nominal yield (obtained using the POWHEG generator interfaced to PYTHIA) with the equivalent result with a different set of generators (MC@NLO simulation for the s - and Wt -channels and ACERMC [70] for the generation of t -channel events). The effect of the (MC) top-quark mass used in the single-top background evaluation is also estimated by using two different input masses: 172.5 and 175 GeV, as well as differences in the kinematics of the single top events. The uncertainty quoted as *background* in table 3 is calculated as the quadratic sum of all the above contributions.

Table 3 summarizes all uncertainties on the estimated top-quark pole mass.

Description	Value [GeV]	%
m_t^{pole}	173.71	
Statistical uncertainty	1.50	0.9
Scale variations	(+0.93, -0.44)	(+0.5, -0.3)
Proton PDF (theory) and α_s	0.21	0.1
Total theory systematic uncertainty	(+0.95, -0.49)	(+0.5, -0.3)
Jet energy scale (including b -jet energy scale)	0.94	0.5
Jet energy resolution	0.02	< 0.1
Jet reconstruction efficiency	0.05	< 0.1
b -tagging efficiency and mistag rate	0.17	0.1
Lepton uncertainties	0.07	< 0.1
Missing transverse momentum	0.02	0.1
MC statistics	0.13	< 0.1
Signal MC generator	0.28	0.2
Hadronization	0.33	0.2
ISR/FSR	0.72	0.4
Colour reconnection	0.14	< 0.1
Underlying event	0.25	0.1
Proton PDF (experimental)	0.54	0.3
Background	0.20	0.1
Total experimental systematic uncertainty	1.44	0.8
Total uncertainty	(+2.29, -2.14)	(+1.3, -1.2)

Table 3. Value of the inferred top-quark pole mass and breakdown of their associated uncertainties.

8.5 Studies on the definition of the extra jet

The extra jet of the $t\bar{t} + 1$ -jet system is required to have a p_T larger than 50 GeV but other possibilities were also investigated. The full analysis was repeated with the p_T of the extra jet satisfying different conditions such as $p_T > 30$ GeV and $p_T > 40$ GeV. The results differ from the baseline central value by less than 0.1 GeV but the change in the systematic and statistical precision of the measurements was significant. As the p_T requirement was decreased some systematics uncertainties, such as that due to the JES, increased and the statistical uncertainty became smaller. The original p_T condition of 50 GeV represents a good compromise for the overall balance of these uncertainties and therefore was used as the baseline of the analysis.

ρ_s interval	\mathcal{R}	Stat. Unc. (%)	Syst. Unc. (%)
0 to 0.25	0.126	12.8	7.1
0.25 to 0.325	1.122	6.6	4.5
0.325 to 0.425	2.049	5.0	3.5
0.425 to 0.525	2.622	4.6	2.1
0.525 to 0.675	2.125	4.1	3.1
0.675 to 1.0	0.302	8.2	8.1

Table 4. Measured values of the \mathcal{R} -distribution and their experimental uncertainties in percent. The statistical uncertainties are derived from the covariance matrix of eq. (7.5).

8.6 Uncertainties on the measured \mathcal{R} -distribution

The experimental uncertainties of the unfolded \mathcal{R} -distribution for each interval of ρ_s are listed in table 4. These uncertainties are obtained following the same methodology as described in previous sections for the top-quark mass but this time applied to the \mathcal{R} -distribution. For each bin of the \mathcal{R} -distribution, all uncertainties have been added in quadrature.

9 Results and discussion

This paper describes an experimental measurement of the top-quark mass using the novel method proposed in ref. [13]. The value of m_t^{pole} is obtained from a fit to the normalized differential cross section $\mathcal{R}(m_t^{\text{pole}}, \rho_s)$ for $t\bar{t}$ production with at least one extra jet, $t\bar{t} + 1\text{-jet}$, as a function of the inverse of the invariant mass of the $t\bar{t} + 1\text{-jet}$ system, ρ_s . This method allows a rigorous theoretical interpretation of the extracted mass parameter in terms of the top-quark pole mass or the running mass in the $\overline{\text{MS}}$ scheme. In the present analysis only the top-quark pole mass (m_t^{pole}) is measured, although future studies should also be able to determine the running mass when the theoretical calculations become available.

Events with the $t\bar{t} + 1\text{-jet}$ final state were selected using 4.6 fb^{-1} of 7 TeV pp collision data collected by the ATLAS experiment at the LHC in 2011. The total background in the $t\bar{t} + 1\text{-jet}$ sample is $\sim 6\%$. Many distributions were studied to demonstrate the overall agreement between the MC predictions and data. A thorough study of the systematic effects with impact on the measurement was carried out and the associated uncertainties quantified. Experimental systematic uncertainties were computed for detector, signal and background modelling.

The measured top-quark pole mass is:

$$m_t^{\text{pole}} = 173.7 \pm 1.5 \text{ (stat.)} \pm 1.4 \text{ (syst.)}_{-0.5}^{+1.0} \text{ (theory) GeV,}$$

where the theoretical uncertainties include the uncertainty due to missing higher orders in the perturbative NLO calculation, as well as uncertainties due to the PDF and α_s used in the calculations. The experimental uncertainty accounts for the uncertainties due to

the imperfections in the modelling of the detector response, the background yield and the uncertainties arising from the signal modelling including hadronization. The dominant experimental uncertainties are due to the jet energy calibration (0.94 GeV) and the initial- and final-state radiation modelling (0.72 GeV).

This measurement constitutes the first extraction of the top-quark pole mass from a measurement of the differential $t\bar{t}+1$ -jet production cross section as a function of the inverse of the invariant mass of the $t\bar{t}+1$ -jet system. It represents the most precise measurement of the top-quark pole mass to date with a total uncertainty of +2.3 GeV and -2.1 GeV. The value obtained for the top-quark pole mass agrees with the most accurate previous top-quark mass measurement in the pole-mass scheme [11] and with the direct top-quark mass measurement [6].

The analysis presented in this paper is statistically uncorrelated from the m_t^{pole} measurement using the inclusive cross-section measured in dilepton events [11]. The measurements could therefore potentially be combined, however this would require a detailed study of the correlations of both the uncertainties on the experimental measurements and the theoretical calculations.

Acknowledgments

We are very grateful to S. Alioli, S. Moch and P. Uwer for their fruitful collaboration in developing the theoretical aspects of the analysis presented in this paper and for their continuous support in implementing the new methodology in the experimental analysis.

We thank CERN for the very successful operation of the LHC, as well as the support staff from our institutions without whom ATLAS could not be operated efficiently.

We acknowledge the support of ANPCyT, Argentina; YerPhI, Armenia; ARC, Australia; BMWF and FWF, Austria; ANAS, Azerbaijan; SSTC, Belarus; CNPq and FAPESP, Brazil; NSERC, NRC and CFI, Canada; CERN; CONICYT, Chile; CAS, MOST and NSFC, China; COLCIENCIAS, Colombia; MSMT CR, MPO CR and VSC CR, Czech Republic; D NRF, DNSRC and Lundbeck Foundation, Denmark; EPLANET, ERC and NSRF, European Union; IN2P3-CNRS, CEA-DSM/IRFU, France; GNSF, Georgia; BMBF, DFG, HGF, MPG and AvH Foundation, Germany; GSRT and NSRF, Greece; ISF, MINERVA, GIF, I-CORE and Benoziyo Center, Israel; INFN, Italy; MEXT and JSPS, Japan; CNRST, Morocco; FOM and NWO, Netherlands; BRF and RCN, Norway; MNiSW and NCN, Poland; GRICES and FCT, Portugal; MNE/IFA, Romania; MES of Russia and ROSATOM, Russian Federation; JINR; MSTD, Serbia; MSSR, Slovakia; ARRS and MIZŠ, Slovenia; DST/NRF, South Africa; MINECO, Spain; SRC and Wallenberg Foundation, Sweden; SER, SNSF and Cantons of Bern and Geneva, Switzerland; NSC, Taiwan; TAEK, Turkey; STFC, the Royal Society and Leverhulme Trust, United Kingdom; DOE and NSF, United States of America.

The crucial computing support from all WLCG partners is acknowledged gratefully, in particular from CERN and the ATLAS Tier-1 facilities at TRIUMF (Canada), NDGF (Denmark, Norway, Sweden), CC-IN2P3 (France), KIT/GridKA (Germany), INFN-CNAF (Italy), NL-T1 (Netherlands), PIC (Spain), ASGC (Taiwan), RAL (U.K.) and BNL (U.S.A.) and in the Tier-2 facilities worldwide.

Open Access. This article is distributed under the terms of the Creative Commons Attribution License ([CC-BY 4.0](https://creativecommons.org/licenses/by/4.0/)), which permits any use, distribution and reproduction in any medium, provided the original author(s) and source are credited.

References

- [1] GFITTER GROUP collaboration, M. Baak et al., *The global electroweak fit at NNLO and prospects for the LHC and ILC*, *Eur. Phys. J. C* **74** (2014) 3046 [[arXiv:1407.3792](https://arxiv.org/abs/1407.3792)] [[INSPIRE](#)].
- [2] S. Moch et al., *High precision fundamental constants at the TeV scale*, [arXiv:1405.4781](https://arxiv.org/abs/1405.4781) [[INSPIRE](#)].
- [3] G. Degrandi et al., *Higgs mass and vacuum stability in the Standard Model at NNLO*, *JHEP* **08** (2012) 098 [[arXiv:1205.6497](https://arxiv.org/abs/1205.6497)] [[INSPIRE](#)].
- [4] S. Alekhin, A. Djouadi and S. Moch, *The top quark and Higgs boson masses and the stability of the electroweak vacuum*, *Phys. Lett. B* **716** (2014) 214 [[arXiv:1207.0980](https://arxiv.org/abs/1207.0980)] [[INSPIRE](#)].
- [5] D. Buttazzo et al., *Investigating the near-criticality of the Higgs boson*, *JHEP* **12** (2013) 089 [[arXiv:1307.3536](https://arxiv.org/abs/1307.3536)] [[INSPIRE](#)].
- [6] ATLAS, CDF, CMS and D0 collaborations, *First combination of Tevatron and LHC measurements of the top-quark mass*, *ATLAS-CONF-2014-008*, CERN, Geneva Switzerland (2014) [CDF-NOTE-1107] [CMS-PAS-TOP-13-014] [D0-NOTE-6416].
- [7] A.H. Hoang and I.W. Stewart, *Top-mass measurements from jets and the Tevatron top mass*, *Nuovo Cim. B* **123** (2008) 1092 [[INSPIRE](#)].
- [8] A. Buckley et al., *General-purpose event generators for LHC physics*, *Phys. Rept.* **504** (2011) 145 [[arXiv:1101.2599](https://arxiv.org/abs/1101.2599)] [[INSPIRE](#)].
- [9] A.H. Hoang, *The top mass: interpretation and theoretical uncertainties*, [arXiv:1412.3649](https://arxiv.org/abs/1412.3649) [[INSPIRE](#)].
- [10] U. Langenfeld, S. Moch and P. Uwer, *Measuring the running top-quark mass*, *Phys. Rev. D* **80** (2009) 054009 [[arXiv:0906.5273](https://arxiv.org/abs/0906.5273)] [[INSPIRE](#)].
- [11] ATLAS collaboration, *Measurement of the $t\bar{t}$ production cross-section using $e\mu$ events with b -tagged jets in pp collisions at $\sqrt{s} = 7$ and 8 TeV with the ATLAS detector*, *Eur. Phys. J. C* **74** (2014) 3109 [[arXiv:1406.5375](https://arxiv.org/abs/1406.5375)] [[INSPIRE](#)].
- [12] CMS collaboration, *Determination of the top-quark pole mass and strong coupling constant from the $t\bar{t}$ production cross section in pp collisions at $\sqrt{s} = 7$ TeV*, *Phys. Lett. B* **728** (2014) 496 [*Erratum ibid.* **728** (2014) 526] [[arXiv:1307.1907](https://arxiv.org/abs/1307.1907)] [[INSPIRE](#)].
- [13] S. Alioli et al., *A new observable to measure the top-quark mass at hadron colliders*, *Eur. Phys. J. C* **73** (2013) 2438 [[arXiv:1303.6415](https://arxiv.org/abs/1303.6415)] [[INSPIRE](#)].
- [14] ATLAS collaboration, *The ATLAS experiment at the CERN Large Hadron Collider*, *2008 JINST* **3** S08003 [[INSPIRE](#)].
- [15] ATLAS collaboration, *Improved luminosity determination in pp collisions at $\sqrt{s} = 7$ TeV using the ATLAS detector at the LHC*, *Eur. Phys. J. C* **73** (2013) 2518 [[arXiv:1302.4393](https://arxiv.org/abs/1302.4393)] [[INSPIRE](#)].
- [16] S. Dittmaier, P. Uwer and S. Weinzierl, *NLO QCD corrections to $t\bar{t} +$ jet production at hadron colliders*, *Phys. Rev. Lett.* **98** (2007) 262002 [[hep-ph/0703120](https://arxiv.org/abs/hep-ph/0703120)] [[INSPIRE](#)].
- [17] S. Dittmaier, P. Uwer and S. Weinzierl, *Hadronic top-quark pair production in association with a hard jet at next-to-leading order QCD: phenomenological studies for the Tevatron and the LHC*, *Eur. Phys. J. C* **59** (2009) 625 [[arXiv:0810.0452](https://arxiv.org/abs/0810.0452)] [[INSPIRE](#)].

- [18] S. Alioli, S.-O. Moch and P. Uwer, *Hadronic top-quark pair-production with one jet and parton showering*, *JHEP* **01** (2012) 137 [[arXiv:1110.5251](#)] [[INSPIRE](#)].
- [19] M. Cacciari, G.P. Salam and G. Soyez, *The anti- k_t jet clustering algorithm*, *JHEP* **04** (2008) 063 [[arXiv:0802.1189](#)] [[INSPIRE](#)].
- [20] M. Cacciari, G.P. Salam and G. Soyez, *FastJet user manual*, *Eur. Phys. J. C* **72** (2012) 1896 [[arXiv:1111.6097](#)] [[INSPIRE](#)].
- [21] S. Frixione, P. Nason and C. Oleari, *Matching NLO QCD computations with parton shower simulations: the POWHEG method*, *JHEP* **11** (2007) 070 [[arXiv:0709.2092](#)] [[INSPIRE](#)].
- [22] S. Alioli, P. Nason, C. Oleari and E. Re, *A general framework for implementing NLO calculations in shower Monte Carlo programs: the POWHEG BOX*, *JHEP* **06** (2010) 043 [[arXiv:1002.2581](#)] [[INSPIRE](#)].
- [23] T. Sjöstrand, S. Mrenna and P.Z. Skands, *A brief introduction to PYTHIA 8.1*, *Comput. Phys. Commun.* **178** (2008) 852 [[arXiv:0710.3820](#)] [[INSPIRE](#)].
- [24] T. Sjöstrand, S. Mrenna and P.Z. Skands, *PYTHIA 6.4 physics and manual*, *JHEP* **05** (2006) 026 [[hep-ph/0603175](#)] [[INSPIRE](#)].
- [25] A. Denner, S. Dittmaier, S. Kallweit and S. Pozzorini, *NLO QCD corrections to off-shell top-antitop production with leptonic decays at hadron colliders*, *JHEP* **10** (2012) 110 [[arXiv:1207.5018](#)] [[INSPIRE](#)].
- [26] A. Denner, S. Dittmaier, S. Kallweit and S. Pozzorini, *NLO QCD corrections to WWbb production at hadron colliders*, *Phys. Rev. Lett.* **106** (2011) 052001 [[arXiv:1012.3975](#)] [[INSPIRE](#)].
- [27] S. Frixione, P. Nason and G. Ridolfi, *A Positive-weight next-to-leading-order Monte Carlo for heavy flavour hadroproduction*, *JHEP* **09** (2007) 126 [[arXiv:0707.3088](#)] [[INSPIRE](#)].
- [28] H.-L. Lai et al., *New parton distributions for collider physics*, *Phys. Rev. D* **82** (2010) 074024 [[arXiv:1007.2241](#)] [[INSPIRE](#)].
- [29] P.Z. Skands, *Tuning Monte Carlo generators: the Perugia tunes*, *Phys. Rev. D* **82** (2010) 074018 [[arXiv:1005.3457](#)] [[INSPIRE](#)].
- [30] M. Cacciari, M. Czakon, M. Mangano, A. Mitov and P. Nason, *Top-pair production at hadron colliders with next-to-next-to-leading logarithmic soft-gluon resummation*, *Phys. Lett. B* **710** (2014) 612 [[arXiv:1111.5869](#)] [[INSPIRE](#)].
- [31] P. Bärnreuther, M. Czakon and A. Mitov, *Percent level precision physics at the Tevatron: first genuine NNLO QCD corrections to $q\bar{q} \rightarrow t\bar{t} + X$* , *Phys. Rev. Lett.* **109** (2012) 132001 [[arXiv:1204.5201](#)] [[INSPIRE](#)].
- [32] M. Czakon and A. Mitov, *NNLO corrections to top pair production at hadron colliders: the quark-gluon reaction*, *JHEP* **01** (2013) 080 [[arXiv:1210.6832](#)] [[INSPIRE](#)].
- [33] M. Czakon, P. Fiedler and A. Mitov, *Total top-quark pair-production cross section at hadron colliders through $O(\alpha_s^4)$* , *Phys. Rev. Lett.* **110** (2013) 252004 [[arXiv:1303.6254](#)] [[INSPIRE](#)].
- [34] M. Czakon and A. Mitov, *Top++: a program for the calculation of the top-pair cross-section at hadron colliders*, *Comput. Phys. Commun.* **185** (2014) 2930 [[arXiv:1112.5675](#)] [[INSPIRE](#)].
- [35] M.L. Mangano, M. Moretti, F. Piccinini, R. Pittau and A.D. Polosa, *ALPGEN, a generator for hard multiparton processes in hadronic collisions*, *JHEP* **07** (2003) 001 [[hep-ph/0206293](#)] [[INSPIRE](#)].

- [36] J. Pumplin, D.R. Stump, J. Huston, H.L. Lai, P.M. Nadolsky and W.K. Tung, *New generation of parton distributions with uncertainties from global QCD analysis*, *JHEP* **07** (2002) 012 [[hep-ph/0201195](#)] [[INSPIRE](#)].
- [37] G. Corcella et al., *HERWIG 6: an event generator for hadron emission reactions with interfering gluons (including supersymmetric processes)*, *JHEP* **01** (2001) 010 [[hep-ph/0011363](#)] [[INSPIRE](#)].
- [38] J.M. Butterworth, J.R. Forshaw and M.H. Seymour, *Multiparton interactions in photoproduction at HERA*, *Z. Phys. C* **72** (1996) 637 [[hep-ph/9601371](#)] [[INSPIRE](#)].
- [39] ATLAS collaboration, *Measurement of the charge asymmetry in top quark pair production in pp collisions at $\sqrt{s} = 7$ TeV using the ATLAS detector*, *Eur. Phys. J. C* **72** (2012) 2039 [[arXiv:1203.4211](#)] [[INSPIRE](#)].
- [40] A. Sherstnev and R.S. Thorne, *Parton distributions for LO generators*, *Eur. Phys. J. C* **55** (2008) 553 [[arXiv:0711.2473](#)] [[INSPIRE](#)].
- [41] ATLAS collaboration, *Measurement of the top quark-pair production cross section with ATLAS in pp collisions at $\sqrt{s} = 7$ TeV*, *Eur. Phys. J. C* **71** (2011) 1577 [[arXiv:1012.1792](#)] [[INSPIRE](#)].
- [42] ATLAS collaboration, *ATLAS tunes of PYTHIA 6 and PYTHIA 8 for MC11*, [ATL-PHYS-PUB-2011-009](#), CERN, Geneva Switzerland (2011).
- [43] ATLAS collaboration, *The ATLAS simulation infrastructure*, *Eur. Phys. J. C* **70** (2010) 823 [[arXiv:1005.4568](#)] [[INSPIRE](#)].
- [44] GEANT4 collaboration, S. Agostinelli et al., *GEANT4: a simulation toolkit*, *Nucl. Instrum. Meth. A* **506** (2003) 250 [[INSPIRE](#)].
- [45] ATLAS collaboration, *Electron reconstruction and identification efficiency measurements with the ATLAS detector using the 2011 LHC proton-proton collision data*, *Eur. Phys. J. C* **74** (2014) 2941 [[arXiv:1404.2240](#)] [[INSPIRE](#)].
- [46] ATLAS collaboration, *Muon reconstruction efficiency and momentum resolution of the ATLAS experiment in proton-proton collisions at $\sqrt{s} = 7$ TeV in 2010*, *Eur. Phys. J. C* **74** (2014) 3034 [[arXiv:1404.4562](#)] [[INSPIRE](#)].
- [47] ATLAS collaboration, *Measurement of the muon reconstruction performance of the ATLAS detector using 2011 and 2012 LHC proton-proton collision data*, *Eur. Phys. J. C* **74** (2014) 3130 [[arXiv:1407.3935](#)] [[INSPIRE](#)].
- [48] ATLAS collaboration, *Measurement of the top quark pair production cross section in pp collisions at $\sqrt{s} = 7$ TeV in dilepton final states with ATLAS*, *Phys. Lett. B* **707** (2013) 459 [[arXiv:1108.3699](#)] [[INSPIRE](#)].
- [49] W. Lampl et al., *Calorimeter clustering algorithms: description and performance*, [ATL-LARG-PUB-2008-002](#), CERN, Geneva Switzerland (2008) [[ATL-COM-LARG-2008-003](#)].
- [50] ATLAS collaboration, *Jet energy measurement and its systematic uncertainty in proton-proton collisions at $\sqrt{s} = 7$ TeV with the ATLAS detector*, *Eur. Phys. J. C* **75** (2015) 17 [[arXiv:1406.0076](#)] [[INSPIRE](#)].
- [51] ATLAS collaboration, *Performance of primary vertex reconstruction in proton-proton collisions at $\sqrt{s} = 7$ TeV in the ATLAS experiment*, [ATLAS-CONF-2010-069](#), CERN, Geneva Switzerland (2010).
- [52] ATLAS collaboration, *Measurement of the mistag rate with 5 fb^{-1} of data collected by the ATLAS detector*, [ATLAS-CONF-2012-040](#), CERN, Geneva Switzerland (2012).

- [53] ATLAS collaboration, *Measurement of the b-tag efficiency in a sample of jets containing muons with 5 fb^{-1} of data from the ATLAS detector*, [ATLAS-CONF-2012-043](#), CERN, Geneva Switzerland (2012).
- [54] ATLAS collaboration, *Measuring the b-tag efficiency in a top-pair sample with 4.7 fb^{-1} of data from the ATLAS detector*, [ATLAS-CONF-2012-097](#), CERN, Geneva Switzerland (2012).
- [55] ATLAS collaboration, *Performance of missing transverse momentum reconstruction in proton-proton collisions at 7 TeV with ATLAS*, *Eur. Phys. J. C* **72** (2012) 1844 [[arXiv:1108.5602](#)] [[INSPIRE](#)].
- [56] PARTICLE DATA GROUP collaboration, K.A. Olive et al., *Review of particle physics*, *Chin. Phys. C* **38** (2014) 090001 [[INSPIRE](#)].
- [57] ATLAS collaboration, *Measurements of normalized differential cross sections for $t\bar{t}$ production in pp collisions at $\sqrt{s} = 7\text{ TeV}$ using the ATLAS detector*, *Phys. Rev. D* **90** (2014) 072004 [[arXiv:1407.0371](#)] [[INSPIRE](#)].
- [58] A. Hocker and V. Kartvelishvili, *SVD approach to data unfolding*, *Nucl. Instrum. Meth. A* **372** (1996) 469 [[hep-ph/9509307](#)] [[INSPIRE](#)].
- [59] J. Gao et al., *CT10 next-to-next-to-leading order global analysis of QCD*, *Phys. Rev. D* **89** (2014) 033009 [[arXiv:1302.6246](#)] [[INSPIRE](#)].
- [60] A.D. Martin, W.J. Stirling, R.S. Thorne and G. Watt, *Parton distributions for the LHC*, *Eur. Phys. J. C* **63** (2009) 189 [[arXiv:0901.0002](#)] [[INSPIRE](#)].
- [61] A.D. Martin, W.J. Stirling, R.S. Thorne and G. Watt, *Uncertainties on α_s in global PDF analyses and implications for predicted hadronic cross sections*, *Eur. Phys. J. C* **64** (2009) 653 [[arXiv:0905.3531](#)] [[INSPIRE](#)].
- [62] R.D. Ball et al., *Parton distributions with LHC data*, *Nucl. Phys. B* **867** (2013) 244 [[arXiv:1207.1303](#)] [[INSPIRE](#)].
- [63] ATLAS collaboration, *Jet energy measurement with the ATLAS detector in proton-proton collisions at $\sqrt{s} = 7\text{ TeV}$* , *Eur. Phys. J. C* **73** (2013) 2304 [[arXiv:1112.6426](#)] [[INSPIRE](#)].
- [64] ATLAS collaboration, *Jet energy resolution in proton-proton collisions at $\sqrt{s} = 7\text{ TeV}$ recorded in 2010 with the ATLAS detector*, *Eur. Phys. J. C* **73** (2013) 2306 [[arXiv:1210.6210](#)] [[INSPIRE](#)].
- [65] S. Frixione, F. Stoeckli, P. Torrielli, B.R. Webber and C.D. White, *The MC@NLO 4.0 event generator*, [arXiv:1010.0819](#) [[INSPIRE](#)].
- [66] ATLAS collaboration, *Measurement of $t\bar{t}$ production with a veto on additional central jet activity in pp collisions at $\sqrt{s} = 7\text{ TeV}$ using the ATLAS detector*, *Eur. Phys. J. C* **72** (2012) 2043 [[arXiv:1203.5015](#)] [[INSPIRE](#)].
- [67] P.Z. Skands, *Tuning Monte Carlo generators: the Perugia tunes*, *Phys. Rev. D* **82** (2010) 074018 [[arXiv:1005.3457](#)] [[INSPIRE](#)].
- [68] M. Botje et al., *The PDF4LHC working group interim recommendations*, [arXiv:1101.0538](#) [[INSPIRE](#)].
- [69] J. Alwall et al., *Comparative study of various algorithms for the merging of parton showers and matrix elements in hadronic collisions*, *Eur. Phys. J. C* **53** (2008) 473 [[arXiv:0706.2569](#)] [[INSPIRE](#)].
- [70] B.P. Kersevan and E. Richter-Was, *The Monte Carlo event generator AcerMC versions 2.0 to 3.8 with interfaces to PYTHIA 6.4, HERWIG 6.5 and ARIADNE 4.1*, *Comput. Phys. Commun.* **184** (2013) 919 [[hep-ph/0405247](#)] [[INSPIRE](#)].

The ATLAS collaboration

G. Aad⁸⁵, B. Abbott¹¹³, J. Abdallah¹⁵², S. Abdel Khalek¹¹⁷, O. Abdinov¹¹, R. Aben¹⁰⁷, B. Abi¹¹⁴, M. Abolins⁹⁰, O.S. AbouZeid¹⁵⁹, H. Abramowicz¹⁵⁴, H. Abreu¹⁵³, R. Abreu³⁰, Y. Abulaiti^{147a,147b}, B.S. Acharya^{165a,165b,a}, L. Adamczyk^{38a}, D.L. Adams²⁵, J. Adelman¹⁰⁸, S. Adomeit¹⁰⁰, T. Adye¹³¹, T. Agatonovic-Jovin¹³, J.A. Aguilar-Saavedra^{126a,126f}, M. Agustoni¹⁷, S.P. Ahlen²², F. Ahmadov^{65,b}, G. Aielli^{134a,134b}, H. Akerstedt^{147a,147b}, T.P.A. Åkesson⁸¹, G. Akimoto¹⁵⁶, A.V. Akimov⁹⁶, G.L. Alberghi^{20a,20b}, J. Albert¹⁷⁰, S. Albrand⁵⁵, M.J. Alconada Verzini⁷¹, M. Aleksa³⁰, I.N. Aleksandrov⁶⁵, C. Alexa^{26a}, G. Alexander¹⁵⁴, T. Alexopoulos¹⁰, M. Alhroob¹¹³, G. Alimonti^{91a}, L. Alio⁸⁵, J. Alison³¹, B.M.M. Allbrooke¹⁸, L.J. Allison⁷², P.P. Allport⁷⁴, A. Aloisio^{104a,104b}, A. Alonso³⁶, F. Alonso⁷¹, C. Alpigiani⁷⁶, A. Altheimer³⁵, B. Alvarez Gonzalez⁹⁰, M.G. Alviggi^{104a,104b}, K. Amako⁶⁶, Y. Amaral Coutinho^{24a}, C. Amelung²³, D. Amidei⁸⁹, S.P. Amor Dos Santos^{126a,126c}, A. Amorim^{126a,126b}, S. Amoroso⁴⁸, N. Amram¹⁵⁴, G. Amundsen²³, C. Anastopoulos¹⁴⁰, L.S. Ancu⁴⁹, N. Andari³⁰, T. Andeen³⁵, C.F. Anders^{58b}, G. Anders³⁰, K.J. Anderson³¹, A. Andreazza^{91a,91b}, V. Andrei^{58a}, X.S. Anduaga⁷¹, S. Angelidakis⁹, I. Angelozzi¹⁰⁷, P. Anger⁴⁴, A. Angerami³⁵, F. Anghinolfi³⁰, A.V. Anisenkov^{109,c}, N. Anjos¹², A. Annovi^{124a,124b}, M. Antonelli⁴⁷, A. Antonov⁹⁸, J. Antos^{145b}, F. Anulli^{133a}, M. Aoki⁶⁶, L. Aperio Bella¹⁸, G. Arabidze⁹⁰, Y. Arai⁶⁶, J.P. Araque^{126a}, A.T.H. Arce⁴⁵, F.A. Arduh⁷¹, J-F. Arguin⁹⁵, S. Argyropoulos⁴², M. Arik^{19a}, A.J. Armbruster³⁰, O. Arnaez³⁰, V. Arnal⁸², H. Arnold⁴⁸, M. Arratia²⁸, O. Arslan²¹, A. Artamonov⁹⁷, G. Artoni²³, S. Asai¹⁵⁶, N. Asbah⁴², A. Ashkenazi¹⁵⁴, B. Åsman^{147a,147b}, L. Asquith¹⁵⁰, K. Assamagan²⁵, R. Astalos^{145a}, M. Atkinson¹⁶⁶, N.B. Atlay¹⁴², B. Auerbach⁶, K. Augsten¹²⁸, M. Aourousseau^{146b}, G. Avolio³⁰, B. Axen¹⁵, M.K. Ayoub¹¹⁷, G. Azuelos^{95,d}, M.A. Baak³⁰, A.E. Baas^{58a}, C. Bacci^{135a,135b}, H. Bachacou¹³⁷, K. Bachas¹⁵⁵, M. Backes³⁰, M. Backhaus³⁰, P. Bagiachi^{133a,133b}, P. Bagnaia^{133a,133b}, Y. Bai^{33a}, T. Bain³⁵, J.T. Baines¹³¹, O.K. Baker¹⁷⁷, P. Balek¹²⁹, T. Balestri¹⁴⁹, F. Balli⁸⁴, E. Banas³⁹, Sw. Banerjee¹⁷⁴, A.A.E. Bannoura¹⁷⁶, H.S. Bansil¹⁸, L. Barak³⁰, E.L. Barberio⁸⁸, D. Barberis^{50a,50b}, M. Barbero⁸⁵, T. Barillari¹⁰¹, M. Barisonzi^{165a,165b}, T. Barklow¹⁴⁴, N. Barlow²⁸, S.L. Barnes⁸⁴, B.M. Barnett¹³¹, R.M. Barnett¹⁵, Z. Barnovska⁵, A. Baroncelli^{135a}, G. Barone⁴⁹, A.J. Barr¹²⁰, F. Barreiro⁸², J. Barreiro Guimarães da Costa⁵⁷, R. Bartoldus¹⁴⁴, A.E. Barton⁷², P. Bartos^{145a}, A. Bassalat¹¹⁷, A. Basye¹⁶⁶, R.L. Bates⁵³, S.J. Batista¹⁵⁹, J.R. Batley²⁸, M. Battaglia¹³⁸, M. Bause^{133a,133b}, F. Bauer¹³⁷, H.S. Bawa^{144,e}, J.B. Beacham¹¹¹, M.D. Beattie⁷², T. Beau⁸⁰, P.H. Beauchemin¹⁶², R. Beccherle^{124a,124b}, P. Bechtel²¹, H.P. Beck^{17,f}, K. Becker¹²⁰, S. Becker¹⁰⁰, M. Beckingham¹⁷¹, C. Becot¹¹⁷, A.J. Beddall^{19c}, A. Beddall^{19c}, V.A. Bednyakov⁶⁵, C.P. Bee¹⁴⁹, L.J. Beemster¹⁰⁷, T.A. Beermann¹⁷⁶, M. Begel²⁵, J.K. Behr¹²⁰, C. Belanger-Champagne⁸⁷, P.J. Bell⁴⁹, W.H. Bell⁴⁹, G. Bella¹⁵⁴, L. Bellagamba^{20a}, A. Bellerive²⁹, M. Bellomo⁸⁶, K. Belotskiy⁹⁸, O. Beltramello³⁰, O. Benary¹⁵⁴, D. Bencheikroun^{136a}, M. Bender¹⁰⁰, K. Bendtz^{147a,147b}, N. Benekos¹⁰, Y. Benhamou¹⁵⁴, E. Benhar Nocchioli⁴⁹, J.A. Benitez Garcia^{160b}, D.P. Benjamin⁴⁵, J.R. Bensinger²³, S. Bentvelsen¹⁰⁷, L. Beresford¹²⁰, M. Beretta⁴⁷, D. Berge¹⁰⁷, E. Bergeaas Kuutmann¹⁶⁷, N. Berger⁵, F. Berghaus¹⁷⁰, J. Beringer¹⁵, C. Bernard²², N.R. Bernard⁸⁶, C. Bernius¹¹⁰, F.U. Bernlochner²¹, T. Berry⁷⁷, P. Berta¹²⁹, C. Bertella⁸³, G. Bertoli^{147a,147b}, F. Bertolucci^{124a,124b}, C. Bertsche¹¹³, D. Bertsche¹¹³, M.I. Besana^{91a}, G.J. Besjes¹⁰⁶, O. Bessidskaia Bylund^{147a,147b}, M. Bessner⁴², N. Besson¹³⁷, C. Betancourt⁴⁸, S. Bethke¹⁰¹, A.J. Bevan⁷⁶, W. Bhimji⁴⁶, R.M. Bianchi¹²⁵, L. Bianchini²³, M. Bianco³⁰, O. Biebel¹⁰⁰, S.P. Bieniek⁷⁸, M. Biglietti^{135a}, J. Bilbao De Mendizabal⁴⁹, H. Bilokon⁴⁷, M. Bindi⁵⁴, S. Binet¹¹⁷, A. Bingul^{19c}, C. Bini^{133a,133b}, C.W. Black¹⁵¹, J.E. Black¹⁴⁴, K.M. Black²², D. Blackburn¹³⁹, R.E. Blair⁶, J.-B. Blanchard¹³⁷, J.E. Blanco⁷⁷, T. Blazek^{145a}, I. Bloch⁴², C. Blocker²³, W. Blum^{83,*}, U. Blumenschein⁵⁴, G.J. Bobbink¹⁰⁷,

V.S. Bobrovnikov^{109,c}, S.S. Bocchetta⁸¹, A. Bocci⁴⁵, C. Bock¹⁰⁰, M. Boehler⁴⁸, J.A. Bogaerts³⁰, A.G. Bogdanchikov¹⁰⁹, C. Boehm^{147a}, V. Boisvert⁷⁷, T. Bold^{38a}, V. Boldea^{26a}, A.S. Boldyrev⁹⁹, M. Bomben⁸⁰, M. Bona⁷⁶, M. Boonekamp¹³⁷, A. Borisov¹³⁰, G. Borissov⁷², S. Borroni⁴², J. Bortfeldt¹⁰⁰, V. Bortolotto^{60a,60b,60c}, K. Bos¹⁰⁷, D. Boscherini^{20a}, M. Bosman¹², J. Boudreau¹²⁵, J. Bouffard², E.V. Bouhova-Thacker⁷², D. Boumediene³⁴, C. Bourdarios¹¹⁷, N. Bousson¹¹⁴, S. Boutouil^{136d}, A. Boveia³⁰, J. Boyd³⁰, I.R. Boyko⁶⁵, I. Bozic¹³, J. Bracinik¹⁸, A. Brandt⁸, G. Brandt¹⁵, O. Brandt^{58a}, U. Bratzler¹⁵⁷, B. Brau⁸⁶, J.E. Brau¹¹⁶, H.M. Braun^{176,*}, S.F. Brazzale^{165a,165c}, K. Brendlinger¹²², A.J. Brennan⁸⁸, L. Brenner¹⁰⁷, R. Brenner¹⁶⁷, S. Bressler¹⁷³, K. Bristow^{146c}, T.M. Bristow⁴⁶, D. Britton⁵³, D. Britzger⁴², F.M. Brochu²⁸, I. Brock²¹, R. Brock⁹⁰, J. Bronner¹⁰¹, G. Brooijmans³⁵, T. Brooks⁷⁷, W.K. Brooks^{32b}, J. Brosamer¹⁵, E. Brost¹¹⁶, J. Brown⁵⁵, P.A. Bruckman de Renstrom³⁹, D. Bruncko^{145b}, R. Bruneliere⁴⁸, A. Bruni^{20a}, G. Bruni^{20a}, M. Bruschi^{20a}, L. Bryngemark⁸¹, T. Buanes¹⁴, Q. Buat¹⁴³, P. Buchholz¹⁴², A.G. Buckley⁵³, S.I. Buda^{26a}, I.A. Budagov⁶⁵, F. Buehrer⁴⁸, L. Bugge¹¹⁹, M.K. Bugge¹¹⁹, O. Bulekov⁹⁸, H. Burckhart³⁰, S. Burdin⁷⁴, B. Burghgrave¹⁰⁸, S. Burke¹³¹, I. Burmeister⁴³, E. Busato³⁴, D. Büscher⁴⁸, V. Büscher⁸³, P. Bussey⁵³, C.P. Buszello¹⁶⁷, J.M. Butler²², A.I. Butt³, C.M. Buttar⁵³, J.M. Butterworth⁷⁸, P. Butti¹⁰⁷, W. Buttinger²⁵, A. Buzatu⁵³, S. Cabrera Urbán¹⁶⁸, D. Caforio¹²⁸, O. Cakir^{4a}, P. Calafiura¹⁵, A. Calandri¹³⁷, G. Calderini⁸⁰, P. Calfayan¹⁰⁰, L.P. Caloba^{24a}, D. Calvet³⁴, S. Calvet³⁴, R. Camacho Toro⁴⁹, S. Camarda⁴², D. Cameron¹¹⁹, L.M. Caminada¹⁵, R. Caminal Armadans¹², S. Campana³⁰, M. Campanelli⁷⁸, A. Campoverde¹⁴⁹, V. Canale^{104a,104b}, A. Canepa^{160a}, M. Cano Bret⁷⁶, J. Cantero⁸², R. Cantrill^{126a}, T. Cao⁴⁰, M.D.M. Capeans Garrido³⁰, I. Caprini^{26a}, M. Caprini^{26a}, M. Capua^{37a,37b}, R. Caputo⁸³, R. Cardarelli^{134a}, T. Carli³⁰, G. Carlino^{104a}, L. Carminati^{91a,91b}, S. Caron¹⁰⁶, E. Carquin^{32a}, G.D. Carrillo-Montoya⁸, J.R. Carter²⁸, J. Carvalho^{126a,126c}, D. Casadei⁷⁸, M.P. Casado¹², M. Casolino¹², E. Castaneda-Miranda^{146b}, A. Castelli¹⁰⁷, V. Castillo Gimenez¹⁶⁸, N.F. Castro^{126a,g}, P. Catastini⁵⁷, A. Catinaccio³⁰, J.R. Catmore¹¹⁹, A. Cattai³⁰, G. Cattani^{134a,134b}, J. Caudron⁸³, V. Cavaliere¹⁶⁶, D. Cavalli^{91a}, M. Cavalli-Sforza¹², V. Cavasinni^{124a,124b}, F. Ceradini^{135a,135b}, B.C. Cerio⁴⁵, K. Cerny¹²⁹, A.S. Cerqueira^{24b}, A. Cerri¹⁵⁰, L. Cerrito⁷⁶, F. Cerutti¹⁵, M. Cerv³⁰, A. Cervelli¹⁷, S.A. Cetin^{19b}, A. Chafaq^{136a}, D. Chakraborty¹⁰⁸, I. Chalupkova¹²⁹, P. Chang¹⁶⁶, B. Chapleau⁸⁷, J.D. Chapman²⁸, D. Charfeddine¹¹⁷, D.G. Charlton¹⁸, C.C. Chau¹⁵⁹, C.A. Chavez Barajas¹⁵⁰, S. Cheatham¹⁵³, A. Chegwidden⁹⁰, S. Chekanov⁶, S.V. Chekulaev^{160a}, G.A. Chelkov^{65,h}, M.A. Chelstowska⁸⁹, C. Chen⁶⁴, H. Chen²⁵, K. Chen¹⁴⁹, L. Chen^{33d,i}, S. Chen^{33c}, X. Chen^{33f}, Y. Chen⁶⁷, H.C. Cheng⁸⁹, Y. Cheng³¹, A. Cheplakov⁶⁵, E. Cheremushkina¹³⁰, R. Cherkaoui El Moursli^{136e}, V. Chernyatin^{25,*}, E. Cheu⁷, L. Chevalier¹³⁷, V. Chiarella⁴⁷, J.T. Childers⁶, A. Chilingarov⁷², G. Chiodini^{73a}, A.S. Chisholm¹⁸, R.T. Chislett⁷⁸, A. Chitan^{26a}, M.V. Chizhov⁶⁵, K. Choi⁶¹, S. Chouridou⁹, B.K.B. Chow¹⁰⁰, V. Christodoulou⁷⁸, D. Chromek-Burckhart³⁰, M.L. Chu¹⁵², J. Chudoba¹²⁷, A.J. Chuinard⁸⁷, J.J. Chwastowski³⁹, L. Chytka¹¹⁵, G. Ciapetti^{133a,133b}, A.K. Ciftci^{4a}, D. Cinca⁵³, V. Cindro⁷⁵, A. Ciocio¹⁵, Z.H. Citron¹⁷³, M. Ciubancan^{26a}, A. Clark⁴⁹, P.J. Clark⁴⁶, R.N. Clarke¹⁵, W. Cleland¹²⁵, C. Clement^{147a,147b}, Y. Coadou⁸⁵, M. Cobal^{165a,165c}, A. Coccaro¹³⁹, J. Cochran⁶⁴, L. Coffey²³, J.G. Cogan¹⁴⁴, B. Cole³⁵, S. Cole¹⁰⁸, A.P. Colijn¹⁰⁷, J. Collot⁵⁵, T. Colombo^{58c}, G. Compostella¹⁰¹, P. Conde Muiño^{126a,126b}, E. Coniavitis⁴⁸, S.H. Connell^{146b}, I.A. Connolly⁷⁷, S.M. Consonni^{91a,91b}, V. Consorti⁴⁸, S. Constantinescu^{26a}, C. Conta^{121a,121b}, G. Conti³⁰, F. Conventi^{104a,j}, M. Cooke¹⁵, B.D. Cooper⁷⁸, A.M. Cooper-Sarkar¹²⁰, K. Copic¹⁵, T. Cornelissen¹⁷⁶, M. Corradi^{20a}, F. Corriveau^{87,k}, A. Corso-Radu¹⁶⁴, A. Cortes-Gonzalez¹², G. Cortiana¹⁰¹, G. Costa^{91a}, M.J. Costa¹⁶⁸, D. Costanzo¹⁴⁰, D. Côté⁸, G. Cottin²⁸, G. Cowan⁷⁷, B.E. Cox⁸⁴, K. Cranmer¹¹⁰, G. Cree²⁹, S. Crépe-Renaudin⁵⁵, F. Crescioli⁸⁰, W.A. Cribbs^{147a,147b}, M. Crispin Ortuzar¹²⁰, M. Cristinziani²¹, V. Croft¹⁰⁶, G. Crosetti^{37a,37b},

T. Cuhadar Donszelmann¹⁴⁰, J. Cummings¹⁷⁷, M. Curatolo⁴⁷, C. Cuthbert¹⁵¹, H. Czirr¹⁴², P. Czodrowski³, S. D’Auria⁵³, M. D’Onofrio⁷⁴, M.J. Da Cunha Sargedas De Sousa^{126a,126b}, C. Da Via⁸⁴, W. Dabrowski^{38a}, A. Dafinca¹²⁰, T. Dai⁸⁹, O. Dale¹⁴, F. Dallaire⁹⁵, C. Dallapiccola⁸⁶, M. Dam³⁶, J.R. Dandoy³¹, A.C. Daniells¹⁸, M. Danninger¹⁶⁹, M. Dano Hoffmann¹³⁷, V. Dao⁴⁸, G. Darbo^{50a}, S. Darmora⁸, J. Dassoulas³, A. Dattagupta⁶¹, W. Davey²¹, C. David¹⁷⁰, T. Davidek¹²⁹, E. Davies^{120,l}, M. Davies¹⁵⁴, P. Davison⁷⁸, Y. Davygora^{58a}, E. Dawe¹⁴³, I. Dawson¹⁴⁰, R.K. Daya-Ishmukhametova⁸⁶, K. De⁸, R. de Asmundis^{104a}, S. De Castro^{20a,20b}, S. De Cecco⁸⁰, N. De Groot¹⁰⁶, P. de Jong¹⁰⁷, H. De la Torre⁸², F. De Lorenzi⁶⁴, L. De Nooij¹⁰⁷, D. De Pedis^{133a}, A. De Salvo^{133a}, U. De Sanctis¹⁵⁰, A. De Santo¹⁵⁰, J.B. De Vivie De Regie¹¹⁷, W.J. Dearnaley⁷², R. Debbe²⁵, C. Debenedetti¹³⁸, D.V. Dedovich⁶⁵, I. Deigaard¹⁰⁷, J. Del Peso⁸², T. Del Prete^{124a,124b}, D. Delgove¹¹⁷, F. Deliot¹³⁷, C.M. Delitzsch⁴⁹, M. Deliyergiyev⁷⁵, A. Dell’Acqua³⁰, L. Dell’Asta²², M. Dell’Orso^{124a,124b}, M. Della Pietra^{104a,j}, D. della Volpe⁴⁹, M. Delmastro⁵, P.A. Delsart⁵⁵, C. Deluca¹⁰⁷, D.A. DeMarco¹⁵⁹, S. Demers¹⁷⁷, M. Demichev⁶⁵, A. Demilly⁸⁰, S.P. Denisov¹³⁰, D. Derendarz³⁹, J.E. Derkaoui^{136d}, F. Derue⁸⁰, P. Dervan⁷⁴, K. Desch²¹, C. Deterre⁴², P.O. Deviveiros³⁰, A. Dewhurst¹³¹, S. Dhaliwal²³, A. Di Ciaccio^{134a,134b}, L. Di Ciaccio⁵, A. Di Domenico^{133a,133b}, C. Di Donato^{104a,104b}, A. Di Girolamo³⁰, B. Di Girolamo³⁰, A. Di Mattia¹⁵³, B. Di Micco^{135a,135b}, R. Di Nardo⁴⁷, A. Di Simone⁴⁸, R. Di Sipio¹⁵⁹, D. Di Valentino²⁹, C. Diaconu⁸⁵, M. Diamond¹⁵⁹, F.A. Dias⁴⁶, M.A. Diaz^{32a}, E.B. Diehl⁸⁹, J. Dietrich¹⁶, S. Diglio⁸⁵, A. Dimitrievska¹³, J. Dingfelder²¹, P. Dita^{26a}, S. Dita^{26a}, F. Dittus³⁰, F. Djama⁸⁵, T. Djobava^{51b}, J.I. Djuvsland^{58a}, M.A.B. do Vale^{24c}, D. Dobos³⁰, M. Dobre^{26a}, C. Doglioni⁴⁹, T. Dohmae¹⁵⁶, J. Dolejsi¹²⁹, Z. Dolezal¹²⁹, B.A. Dolgoshein^{98,*}, M. Donadelli^{24d}, S. Donati^{124a,124b}, P. Dondero^{121a,121b}, J. Donini³⁴, J. Dopke¹³¹, A. Doria^{104a}, M.T. Dova⁷¹, A.T. Doyle⁵³, E. Drechsler⁵⁴, M. Dris¹⁰, E. Dubreuil³⁴, E. Duchovni¹⁷³, G. Duckeck¹⁰⁰, O.A. Ducu^{26a,85}, D. Duda¹⁷⁶, A. Dudarev³⁰, L. Duflot¹¹⁷, L. Duguid⁷⁷, M. Dührssen³⁰, M. Dunford^{58a}, H. Duran Yildiz^{4a}, M. Düren⁵², A. Durglishvili^{51b}, D. Duschinger⁴⁴, M. Dwuznik^{38a}, M. Dyndal^{38a}, K.M. Ecker¹⁰¹, W. Edson², N.C. Edwards⁴⁶, W. Ehrenfeld²¹, T. Eifert³⁰, G. Eigen¹⁴, K. Einsweiler¹⁵, T. Ekelof¹⁶⁷, M. El Kacimi^{136c}, M. Ellert¹⁶⁷, S. Elles⁵, F. Ellinghaus⁸³, A.A. Elliot¹⁷⁰, N. Ellis³⁰, J. Elmsheuser¹⁰⁰, M. Elsing³⁰, D. Emelianov¹³¹, Y. Enari¹⁵⁶, O.C. Endner⁸³, M. Endo¹¹⁸, J. Erdmann⁴³, A. Ereditato¹⁷, D. Eriksson^{147a}, G. Ernis¹⁷⁶, J. Ernst², M. Ernst²⁵, S. Errede¹⁶⁶, E. Ertel⁸³, M. Escalier¹¹⁷, H. Esch⁴³, C. Escobar¹²⁵, B. Esposito⁴⁷, A.I. Etienvre¹³⁷, E. Etzion¹⁵⁴, H. Evans⁶¹, A. Ezhilov¹²³, L. Fabbri^{20a,20b}, G. Facini³¹, R.M. Fakhruddinov¹³⁰, S. Falciano^{133a}, R.J. Falla⁷⁸, J. Faltova¹²⁹, Y. Fang^{33a}, M. Fanti^{91a,91b}, A. Farbin⁸, A. Farilla^{135a}, T. Farooque¹², S. Farrell¹⁵, S.M. Farrington¹⁷¹, P. Farthouat³⁰, F. Fassi^{136e}, P. Fassnacht³⁰, D. Fassouliotis⁹, A. Favareto^{50a,50b}, L. Fayard¹¹⁷, P. Federic^{145a}, O.L. Fedin^{123,m}, W. Fedorko¹⁶⁹, S. Feigl³⁰, L. Felgioni⁸⁵, C. Feng^{33d}, E.J. Feng⁶, H. Feng⁸⁹, A.B. Fenyuk¹³⁰, P. Fernandez Martinez¹⁶⁸, S. Fernandez Perez³⁰, S. Ferrag⁵³, J. Ferrando⁵³, A. Ferrari¹⁶⁷, P. Ferrari¹⁰⁷, R. Ferrari^{121a}, D.E. Ferreira de Lima⁵³, A. Ferrer¹⁶⁸, D. Ferrere⁴⁹, C. Ferretti⁸⁹, A. Ferretto Parodi^{50a,50b}, M. Fiascaris³¹, F. Fiedler⁸³, A. Filipčić⁷⁵, M. Filipuzzi⁴², F. Filthaut¹⁰⁶, M. Fincke-Keeler¹⁷⁰, K.D. Finelli¹⁵¹, M.C.N. Fiolhais^{126a,126c}, L. Fiorini¹⁶⁸, A. Firan⁴⁰, A. Fischer², C. Fischer¹², J. Fischer¹⁷⁶, W.C. Fisher⁹⁰, E.A. Fitzgerald²³, M. Flechl⁴⁸, I. Fleck¹⁴², P. Fleischmann⁸⁹, S. Fleischmann¹⁷⁶, G.T. Fletcher¹⁴⁰, G. Fletcher⁷⁶, T. Flick¹⁷⁶, A. Floderus⁸¹, L.R. Flores Castillo^{60a}, M.J. Flowerdew¹⁰¹, A. Formica¹³⁷, A. Forti⁸⁴, D. Fournier¹¹⁷, H. Fox⁷², S. Fracchia¹², P. Francavilla⁸⁰, M. Franchini^{20a,20b}, D. Francis³⁰, L. Franconi¹¹⁹, M. Franklin⁵⁷, M. Fraternali^{121a,121b}, D. Freeborn⁷⁸, S.T. French²⁸, F. Friedrich⁴⁴, D. Froidevaux³⁰, J.A. Frost¹²⁰, C. Fukunaga¹⁵⁷, E. Fullana Torregrosa⁸³, B.G. Fulsom¹⁴⁴, J. Fuster¹⁶⁸, C. Gabaldon⁵⁵, O. Gabizon¹⁷⁶, A. Gabrielli^{20a,20b}, A. Gabrielli^{133a,133b}, S. Gadatsch¹⁰⁷,

S. Gadomski⁴⁹, G. Gagliardi^{50a,50b}, P. Gagnon⁶¹, C. Galea¹⁰⁶, B. Galhardo^{126a,126c},
 E.J. Gallas¹²⁰, B.J. Gallop¹³¹, P. Gallus¹²⁸, G. Galster³⁶, K.K. Gan¹¹¹, J. Gao^{33b,85}, Y. Gao⁴⁶,
 Y.S. Gao^{144,e}, F.M. Garay Walls⁴⁶, F. Garbers¹⁷⁷, C. García¹⁶⁸, J.E. García Navarro¹⁶⁸,
 M. Garcia-Sciveres¹⁵, R.W. Gardner³¹, N. Garelli¹⁴⁴, V. Garonne³⁰, C. Gatti⁴⁷, G. Gaudio^{121a},
 B. Gaur¹⁴², L. Gauthier⁹⁵, P. Gauzzi^{133a,133b}, I.L. Gavrilenko⁹⁶, C. Gay¹⁶⁹, G. Gaycken²¹,
 E.N. Gazis¹⁰, P. Ge^{33d}, Z. Gecse¹⁶⁹, C.N.P. Gee¹³¹, D.A.A. Geerts¹⁰⁷, Ch. Geich-Gimbel²¹,
 C. Gemme^{50a}, M.H. Genest⁵⁵, S. Gentile^{133a,133b}, M. George⁵⁴, S. George⁷⁷, D. Gerbaudo¹⁶⁴,
 A. Gershon¹⁵⁴, H. Ghazlane^{136b}, N. Ghodbane³⁴, B. Giacobbe^{20a}, S. Giagu^{133a,133b},
 V. Giangiobbe¹², P. Giannetti^{124a,124b}, F. Gianotti³⁰, B. Gibbard²⁵, S.M. Gibson⁷⁷,
 M. Gilchriese¹⁵, T.P.S. Gillam²⁸, D. Gillberg³⁰, G. Gilles³⁴, D.M. Gingrich^{3,d}, N. Giokaris⁹,
 M.P. Giordani^{165a,165c}, F.M. Giorgi^{20a}, F.M. Giorgi¹⁶, P.F. Giraud¹³⁷, P. Giromini⁴⁷,
 D. Giugni^{91a}, C. Giuliani⁴⁸, M. Giulini^{58b}, B.K. Gjelsten¹¹⁹, S. Gkaitatzis¹⁵⁵, I. Gkialas¹⁵⁵,
 E.L. Gkoukousis¹¹⁷, L.K. Gladilin⁹⁹, C. Glasman⁸², J. Glatzer³⁰, P.C.F. Glaysheer⁴⁶, A. Glazov⁴²,
 M. Goblirsch-Kolb¹⁰¹, J.R. Goddard⁷⁶, J. Godlewski³⁹, S. Goldfarb⁸⁹, T. Golling⁴⁹,
 D. Golubkov¹³⁰, A. Gomes^{126a,126b,126d}, R. Gonçalo^{126a}, J. Goncalves Pinto Firmino Da Costa¹³⁷,
 L. Gonella²¹, S. González de la Hoz¹⁶⁸, G. Gonzalez Parra¹², S. Gonzalez-Sevilla⁴⁹, L. Goossens³⁰,
 P.A. Gorbounov⁹⁷, H.A. Gordon²⁵, I. Gorelov¹⁰⁵, B. Gorini³⁰, E. Gorini^{73a,73b}, A. Gorišek⁷⁵,
 E. Gornicki³⁹, A.T. Goshaw⁴⁵, C. Gössling⁴³, M.I. Gostkin⁶⁵, M. Goughri^{136a}, D. Goujdami^{136c},
 A.G. Goussiou¹³⁹, H.M.X. Grabas¹³⁸, L. Graber⁵⁴, I. Grabowska-Bold^{38a}, P. Grafström^{20a,20b},
 K-J. Grahn⁴², J. Gramling⁴⁹, E. Gramstad¹¹⁹, S. Grancagnolo¹⁶, V. Grassi¹⁴⁹, V. Gratchev¹²³,
 H.M. Gray³⁰, E. Graziani^{135a}, Z.D. Greenwood^{79,n}, K. Gregersen⁷⁸, I.M. Gregor⁴², P. Grenier¹⁴⁴,
 J. Griffiths⁸, A.A. Grillo¹³⁸, K. Grimm⁷², S. Grinstein^{12,o}, Ph. Gris³⁴, J.-F. Grivaz¹¹⁷,
 J.P. Grohs⁴⁴, A. Grohsjean⁴², E. Gross¹⁷³, J. Grosse-Knetter⁵⁴, G.C. Grossi^{134a,134b},
 Z.J. Grout¹⁵⁰, L. Guan^{33b}, J. Guenther¹²⁸, F. Guescini⁴⁹, D. Guest¹⁷⁷, O. Gueta¹⁵⁴,
 E. Guido^{50a,50b}, T. Guillemin¹¹⁷, S. Guindon², U. Gul⁵³, C. Gumpert⁴⁴, J. Guo^{33e}, S. Gupta¹²⁰,
 P. Gutierrez¹¹³, N.G. Gutierrez Ortiz⁵³, C. Gutsche⁴⁴, N. Guttman¹⁵⁴, C. Guyot¹³⁷,
 C. Gwenlan¹²⁰, C.B. Gwilliam⁷⁴, A. Haas¹¹⁰, C. Haber¹⁵, H.K. Hadavand⁸, N. Haddad^{136e},
 P. Haefner²¹, S. Hageböck²¹, Z. Hajduk³⁹, H. Hakobyan¹⁷⁸, M. Haleem⁴², J. Haley¹¹⁴, D. Hall¹²⁰,
 G. Halladjian⁹⁰, G.D. Hallewell⁸⁵, K. Hamacher¹⁷⁶, P. Hamal¹¹⁵, K. Hamano¹⁷⁰, M. Hamer⁵⁴,
 A. Hamilton^{146a}, S. Hamilton¹⁶², G.N. Hamity^{146c}, P.G. Hamnett⁴², L. Han^{33b}, K. Hanagaki¹¹⁸,
 K. Hanawa¹⁵⁶, M. Hance¹⁵, P. Hanke^{58a}, R. Hanna¹³⁷, J.B. Hansen³⁶, J.D. Hansen³⁶,
 P.H. Hansen³⁶, K. Hara¹⁶¹, A.S. Hard¹⁷⁴, T. Harenberg¹⁷⁶, F. Hariri¹¹⁷, S. Harkusha⁹²,
 R.D. Harrington⁴⁶, P.F. Harrison¹⁷¹, F. Hartjes¹⁰⁷, M. Hasegawa⁶⁷, S. Hasegawa¹⁰³,
 Y. Hasegawa¹⁴¹, A. Hasib¹¹³, S. Hassani¹³⁷, S. Haug¹⁷, R. Hauser⁹⁰, L. Hauswald⁴⁴,
 M. Havranek¹²⁷, C.M. Hawkes¹⁸, R.J. Hawkings³⁰, A.D. Hawkins⁸¹, T. Hayashi¹⁶¹, D. Hayden⁹⁰,
 C.P. Hays¹²⁰, J.M. Hays⁷⁶, H.S. Hayward⁷⁴, S.J. Haywood¹³¹, S.J. Head¹⁸, T. Heck⁸³,
 V. Hedberg⁸¹, L. Heelan⁸, S. Heim¹²², T. Heim¹⁷⁶, B. Heinemann¹⁵, L. Heinrich¹¹⁰, J. Hejbal¹²⁷,
 L. Helary²², M. Heller³⁰, S. Hellman^{147a,147b}, D. Hellmich²¹, C. Helsen³⁰, J. Henderson¹²⁰,
 R.C.W. Henderson⁷², Y. Heng¹⁷⁴, C. Hengler⁴², A. Henrichs¹⁷⁷, A.M. Henriques Correia³⁰,
 S. Henrot-Versille¹¹⁷, G.H. Herbert¹⁶, Y. Hernández Jiménez¹⁶⁸, R. Herrberg-Schubert¹⁶,
 G. Herten⁴⁸, R. Hertenberger¹⁰⁰, L. Hervas³⁰, G.G. Hesketh⁷⁸, N.P. Hessey¹⁰⁷, J.W. Hetherly⁴⁰,
 R. Hickling⁷⁶, E. Higón-Rodríguez¹⁶⁸, E. Hill¹⁷⁰, J.C. Hill²⁸, K.H. Hiller⁴², S.J. Hillier¹⁸,
 I. Hinchliffe¹⁵, E. Hines¹²², R.R. Hinman¹⁵, M. Hirose¹⁵⁸, D. Hirschbuehl¹⁷⁶, J. Hobbs¹⁴⁹,
 N. Hod¹⁰⁷, M.C. Hodgkinson¹⁴⁰, P. Hodgson¹⁴⁰, A. Hoecker³⁰, M.R. Hoferkamp¹⁰⁵, F. Hoenig¹⁰⁰,
 M. Hohlfeld⁸³, D. Hohn²¹, T.R. Holmes¹⁵, T.M. Hong¹²², L. Hooft van Huysduynen¹¹⁰,
 W.H. Hopkins¹¹⁶, Y. Horii¹⁰³, A.J. Horton¹⁴³, J.-Y. Hostachy⁵⁵, S. Hou¹⁵², A. Hoummada^{136a},
 J. Howard¹²⁰, J. Howarth⁴², M. Hrabovsky¹¹⁵, I. Hristova¹⁶, J. Hrivnac¹¹⁷, T. Hryn'ova⁵,
 A. Hrynevich⁹³, C. Hsu^{146c}, P.J. Hsu^{152,p}, S.-C. Hsu¹³⁹, D. Hu³⁵, Q. Hu^{33b}, X. Hu⁸⁹, Y. Huang⁴²,

Z. Hubacek³⁰, F. Hubaut⁸⁵, F. Huegging²¹, T.B. Huffman¹²⁰, E.W. Hughes³⁵, G. Hughes⁷², M. Huhtinen³⁰, T.A. Hülsing⁸³, N. Huseynov^{65,b}, J. Huston⁹⁰, J. Huth⁵⁷, G. Iacobucci⁴⁹, G. Iakovidis²⁵, I. Ibragimov¹⁴², L. Iconomidou-Fayard¹¹⁷, E. Ideal¹⁷⁷, Z. Idrissi^{136e}, P. Iengo³⁰, O. Igonkina¹⁰⁷, T. Iizawa¹⁷², Y. Ikegami⁶⁶, K. Ikematsu¹⁴², M. Ikeno⁶⁶, Y. Ilchenko^{31,q}, D. Iliadis¹⁵⁵, N. Ilic¹⁵⁹, Y. Inamaru⁶⁷, T. Ince¹⁰¹, P. Ioannou⁹, M. Iodice^{135a}, K. Iordanidou⁹, V. Ippolito⁵⁷, A. Irles Quiles¹⁶⁸, C. Isaksson¹⁶⁷, M. Ishino⁶⁸, M. Ishitsuka¹⁵⁸, R. Ishmukhametov¹¹¹, C. Issever¹²⁰, S. Istin^{19a}, J.M. Iturbe Ponce⁸⁴, R. Iuppa^{134a,134b}, J. Ivarsson⁸¹, W. Iwanski³⁹, H. Iwasaki⁶⁶, J.M. Izen⁴¹, V. Izzo^{104a}, S. Jabbar³, B. Jackson¹²², M. Jackson⁷⁴, P. Jackson¹, M.R. Jaekel³⁰, V. Jain², K. Jakobs⁴⁸, S. Jakobsen³⁰, T. Jakoubek¹²⁷, J. Jakubek¹²⁸, D.O. Jamin¹⁵², D.K. Jana⁷⁹, E. Jansen⁷⁸, R.W. Jansky⁶², J. Janssen²¹, M. Janus¹⁷¹, G. Jarlskog⁸¹, N. Javadov^{65,b}, T. Javůrek⁴⁸, L. Jeanty¹⁵, J. Jejelava^{51a,r}, G.-Y. Jeng¹⁵¹, D. Jennens⁸⁸, P. Jenni^{48,s}, J. Jentzsch⁴³, C. Jeske¹⁷¹, S. Jézéquel⁵, H. Ji¹⁷⁴, J. Jia¹⁴⁹, Y. Jiang^{33b}, S. Jiggins⁷⁸, J. Jimenez Pena¹⁶⁸, S. Jin^{33a}, A. Jinaru^{26a}, O. Jinnouchi¹⁵⁸, M.D. Joergensen³⁶, P. Johansson¹⁴⁰, K.A. Johns⁷, K. Jon-And^{147a,147b}, G. Jones¹⁷¹, R.W.L. Jones⁷², T.J. Jones⁷⁴, J. Jongmanns^{58a}, P.M. Jorge^{126a,126b}, K.D. Joshi⁸⁴, J. Jovicevic¹⁴⁸, X. Ju¹⁷⁴, C.A. Jung⁴³, P. Jussel⁶², A. Juste Rozas^{12,o}, M. Kaci¹⁶⁸, A. Kaczmarska³⁹, M. Kado¹¹⁷, H. Kagan¹¹¹, M. Kagan¹⁴⁴, S.J. Kahn⁸⁵, E. Kajomovitz⁴⁵, C.W. Kalderon¹²⁰, S. Kama⁴⁰, A. Kamenshchikov¹³⁰, N. Kanaya¹⁵⁶, M. Kaneda³⁰, S. Kaneti²⁸, V.A. Kantserov⁹⁸, J. Kanzaki⁶⁶, B. Kaplan¹¹⁰, A. Kapliy³¹, D. Kar⁵³, K. Karakostas¹⁰, A. Karamaoun³, N. Karastathis^{10,107}, M.J. Kareem⁵⁴, M. Karnevskiy⁸³, S.N. Karpov⁶⁵, Z.M. Karpova⁶⁵, K. Karthik¹¹⁰, V. Kartvelishvili⁷², A.N. Karyukhin¹³⁰, L. Kashif¹⁷⁴, R.D. Kass¹¹¹, A. Kastanas¹⁴, Y. Kataoka¹⁵⁶, A. Katre⁴⁹, J. Katzy⁴², K. Kawagoe⁷⁰, T. Kawamoto¹⁵⁶, G. Kawamura⁵⁴, S. Kazama¹⁵⁶, V.F. Kazanin^{109,c}, M.Y. Kazarinov⁶⁵, R. Keeler¹⁷⁰, R. Kehoe⁴⁰, J.S. Keller⁴², J.J. Kempster⁷⁷, H. Keoshkerian⁸⁴, O. Kepka¹²⁷, B.P. Kerševan⁷⁵, S. Kersten¹⁷⁶, R.A. Keyes⁸⁷, F. Khalil-zada¹¹, H. Khandanyan^{147a,147b}, A. Khanov¹¹⁴, A.G. Kharlamov^{109,c}, A. Khodinov⁹⁸, T.J. Khoo²⁸, V. Khovanskiy⁹⁷, E. Khramov⁶⁵, J. Khubua^{51b,t}, H.Y. Kim⁸, H. Kim^{147a,147b}, S.H. Kim¹⁶¹, Y. Kim³¹, N. Kimura¹⁵⁵, O.M. Kind¹⁶, B.T. King⁷⁴, M. King¹⁶⁸, R.S.B. King¹²⁰, S.B. King¹⁶⁹, J. Kirk¹³¹, A.E. Kiryunin¹⁰¹, T. Kishimoto⁶⁷, D. Kisielewska^{38a}, F. Kiss⁴⁸, K. Kiuchi¹⁶¹, O. Kivernyk¹³⁷, E. Kladiva^{145b}, M.H. Klein³⁵, M. Klein⁷⁴, U. Klein⁷⁴, K. Kleinknecht⁸³, P. Klimek^{147a,147b}, A. Klimentov²⁵, R. Klingenberg⁴³, J.A. Klinger⁸⁴, T. Klioutchnikova³⁰, P.F. Klok¹⁰⁶, E.-E. Kluge^{58a}, P. Kluit¹⁰⁷, S. Kluth¹⁰¹, E. Kneringer⁶², E.B.F.G. Knoops⁸⁵, A. Knue⁵³, D. Kobayashi¹⁵⁸, T. Kobayashi¹⁵⁶, M. Kobel⁴⁴, M. Kocian¹⁴⁴, P. Kodys¹²⁹, T. Koffas²⁹, E. Koffeman¹⁰⁷, L.A. Kogan¹²⁰, S. Kohlmann¹⁷⁶, Z. Kohout¹²⁸, T. Kohriki⁶⁶, T. Koi¹⁴⁴, H. Kolanoski¹⁶, I. Koletsou⁵, A.A. Komar^{96,*}, Y. Komori¹⁵⁶, T. Kondo⁶⁶, N. Kondrashova⁴², K. Köneke⁴⁸, A.C. König¹⁰⁶, S. König⁸³, T. Kono^{66,u}, R. Konoplich^{110,v}, N. Konstantinidis⁷⁸, R. Kopeliansky¹⁵³, S. Koperny^{38a}, L. Köpke⁸³, A.K. Kopp⁴⁸, K. Korcyl³⁹, K. Kordas¹⁵⁵, A. Korn⁷⁸, A.A. Korol^{109,c}, I. Korolkov¹², E.V. Korolkova¹⁴⁰, O. Kortner¹⁰¹, S. Kortner¹⁰¹, T. Kosek¹²⁹, V.V. Kostyukhin²¹, V.M. Kotov⁶⁵, A. Kotwal⁴⁵, A. Kourkouveli-Charalampidi¹⁵⁵, C. Kourkouvelis⁹, V. Kouskoura²⁵, A. Koutsman^{160a}, R. Kowalewski¹⁷⁰, T.Z. Kowalski^{38a}, W. Kozanecki¹³⁷, A.S. Kozhin¹³⁰, V.A. Kramarenko⁹⁹, G. Kramberger⁷⁵, D. Krasnopevtsev⁹⁸, M.W. Krasny⁸⁰, A. Krasznahorkay³⁰, J.K. Kraus²¹, A. Kravchenko²⁵, S. Kreiss¹¹⁰, M. Kretz^{58c}, J. Kretzschmar⁷⁴, K. Kreutzfeldt⁵², P. Krieger¹⁵⁹, K. Krizka³¹, K. Kroeninger⁴³, H. Kroha¹⁰¹, J. Kroll¹²², J. Kröseberg²¹, J. Krstic¹³, U. Kruchonak⁶⁵, H. Krüger²¹, N. Krumnack⁶⁴, Z.V. Krumshteyn⁶⁵, A. Kruse¹⁷⁴, M.C. Kruse⁴⁵, M. Kruskal²², T. Kubota⁸⁸, H. Kucuk⁷⁸, S. Kuday^{4c}, S. Kuehn⁴⁸, A. Kugel^{58c}, F. Kuger¹⁷⁵, A. Kuhl¹³⁸, T. Kuhl⁴², V. Kukhtin⁶⁵, Y. Kulchitsky⁹², S. Kuleshov^{32b}, M. Kuna^{133a,133b}, T. Kunigo⁶⁸, A. Kupco¹²⁷, H. Kurashige⁶⁷, Y.A. Kurochkin⁹², R. Kurumida⁶⁷, V. Kus¹²⁷, E.S. Kuwertz¹⁴⁸, M. Kuze¹⁵⁸, J. Kvita¹¹⁵, T. Kwan¹⁷⁰, D. Kyriazopoulos¹⁴⁰, A. La Rosa⁴⁹,

J.L. La Rosa Navarro^{24d}, L. La Rotonda^{37a,37b}, C. Lacasta¹⁶⁸, F. Lacava^{133a,133b}, J. Lacey²⁹, H. Lacker¹⁶, D. Lacour⁸⁰, V.R. Lacuesta¹⁶⁸, E. Ladygin⁶⁵, R. Lafaye⁵, B. Laforge⁸⁰, T. Lagouri¹⁷⁷, S. Lai⁴⁸, L. Lambourne⁷⁸, S. Lammers⁶¹, C.L. Lampen⁷, W. Lamp⁷, E. Lançon¹³⁷, U. Landgraf⁴⁸, M.P.J. Landon⁷⁶, V.S. Lang^{58a}, A.J. Lankford¹⁶⁴, F. Lanni²⁵, K. Lantzsch³⁰, S. Laplace⁸⁰, C. Lapoire³⁰, J.F. Laporte¹³⁷, T. Lari^{91a}, F. Lasagni Manghi^{20a,20b}, M. Lassnig³⁰, P. Laurelli⁴⁷, W. Lavrijsen¹⁵, A.T. Law¹³⁸, P. Laycock⁷⁴, O. Le Dortz⁸⁰, E. Le Guirriec⁸⁵, E. Le Menedeu¹², T. LeCompte⁶, F. Ledroit-Guillon⁵⁵, C.A. Lee^{146b}, S.C. Lee¹⁵², L. Lee¹, G. Lefebvre⁸⁰, M. Lefebvre¹⁷⁰, F. Legger¹⁰⁰, C. Leggett¹⁵, A. Lehan⁷⁴, G. Lehmann Miotto³⁰, X. Lei⁷, W.A. Leight²⁹, A. Leisos¹⁵⁵, A.G. Leister¹⁷⁷, M.A.L. Leite^{24d}, R. Leitner¹²⁹, D. Lellouch¹⁷³, B. Lemmer⁵⁴, K.J.C. Leney⁷⁸, T. Lenz²¹, B. Lenzi³⁰, R. Leone⁷, S. Leone^{124a,124b}, C. Leonidopoulos⁴⁶, S. Leontsinis¹⁰, C. Leroy⁹⁵, C.G. Lester²⁸, M. Levchenko¹²³, J. Levêque⁵, D. Levin⁸⁹, L.J. Levinson¹⁷³, M. Levy¹⁸, A. Lewis¹²⁰, A.M. Leyko²¹, M. Leyton⁴¹, B. Li^{33b,w}, B. Li⁸⁵, H. Li¹⁴⁹, H.L. Li³¹, L. Li⁴⁵, L. Li^{33e}, S. Li⁴⁵, Y. Li^{33c,x}, Z. Liang¹³⁸, H. Liao³⁴, B. Libert^{134a}, A. Liblong¹⁵⁹, P. Lichard³⁰, K. Lie¹⁶⁶, J. Liebal²¹, W. Liebig¹⁴, C. Limbach²¹, A. Limosani¹⁵¹, S.C. Lin^{152,y}, T.H. Lin⁸³, F. Linde¹⁰⁷, B.E. Lindquist¹⁴⁹, J.T. Linnemann⁹⁰, E. Lipeles¹²², A. Lipniacka¹⁴, M. Lisovsky⁴², T.M. Liss¹⁶⁶, D. Lissauer²⁵, A. Lister¹⁶⁹, A.M. Litke¹³⁸, B. Liu^{152,z}, D. Liu¹⁵², J. Liu⁸⁵, J.B. Liu^{33b}, K. Liu⁸⁵, L. Liu⁸⁹, M. Liu⁴⁵, M. Liu^{33b}, Y. Liu^{33b}, M. Livan^{121a,121b}, A. Lleres⁵⁵, J. Llorente Merino⁸², S.L. Lloyd⁷⁶, F. Lo Sterzo¹⁵², E. Lobodzinska⁴², P. Loch⁷, W.S. Lockman¹³⁸, F.K. Loebinger⁸⁴, A.E. Loevschall-Jensen³⁶, A. Loginov¹⁷⁷, T. Lohse¹⁶, K. Lohwasser⁴², M. Lokajicek¹²⁷, B.A. Long²², J.D. Long⁸⁹, R.E. Long⁷², K.A. Looper¹¹¹, L. Lopes^{126a}, D. Lopez Mateos⁵⁷, B. Lopez Paredes¹⁴⁰, I. Lopez Paz¹², J. Lorenz¹⁰⁰, N. Lorenzo Martinez⁶¹, M. Losada¹⁶³, P. Loscutoff¹⁵, P.J. Lösel¹⁰⁰, X. Lou^{33a}, A. Lounis¹¹⁷, J. Love⁶, P.A. Love⁷², N. Lu⁸⁹, H.J. Lubatti¹³⁹, C. Luci^{133a,133b}, A. Lucotte⁵⁵, F. Luehring⁶¹, W. Lukas⁶², L. Luminari^{133a}, O. Lundberg^{147a,147b}, B. Lund-Jensen¹⁴⁸, M. Lungwitz⁸³, D. Lynn²⁵, R. Lysak¹²⁷, E. Lytken⁸¹, H. Ma²⁵, L.L. Ma^{33d}, G. Maccarrone⁴⁷, A. Macchiolo¹⁰¹, C.M. Macdonald¹⁴⁰, J. Machado Miguens^{122,126b}, D. Macina³⁰, D. Madaffari⁸⁵, R. Madar³⁴, H.J. Maddocks⁷², W.F. Mader⁴⁴, A. Madsen¹⁶⁷, S. Maeland¹⁴, T. Maeno²⁵, A. Maevskiy⁹⁹, E. Magradze⁵⁴, K. Mahboubi⁴⁸, J. Mahlstedt¹⁰⁷, S. Mahmoud⁷⁴, C. Maiani¹³⁷, C. Maidantchik^{24a}, A.A. Maier¹⁰¹, T. Maier¹⁰⁰, A. Maio^{126a,126b,126d}, S. Majewski¹¹⁶, Y. Makida⁶⁶, N. Makovec¹¹⁷, B. Malaescu⁸⁰, Pa. Malecki³⁹, V.P. Maleev¹²³, F. Malek⁵⁵, U. Mallik⁶³, D. Malon⁶, C. Malone¹⁴⁴, S. Maltezos¹⁰, V.M. Malyshev¹⁰⁹, S. Malyukov³⁰, J. Mamuzic⁴², G. Mancini⁴⁷, B. Mandelli³⁰, L. Mandelli^{91a}, I. Mandić⁷⁵, R. Mandrysch⁶³, J. Maneira^{126a,126b}, A. Manfredini¹⁰¹, L. Manhaes de Andrade Filho^{24b}, J. Manjarres Ramos^{160b}, A. Mann¹⁰⁰, P.M. Manning¹³⁸, A. Manousakis-Katsikakis⁹, B. Mansoulie¹³⁷, R. Mantifel⁸⁷, M. Mantoani⁵⁴, L. Mapelli³⁰, L. March^{146c}, G. Marchiori⁸⁰, M. Marcisovsky¹²⁷, C.P. Marino¹⁷⁰, M. Marjanovic¹³, F. Marroquim^{24a}, S.P. Marsden⁸⁴, Z. Marshall¹⁵, L.F. Marti¹⁷, S. Marti-Garcia¹⁶⁸, B. Martin⁹⁰, T.A. Martin¹⁷¹, V.J. Martin⁴⁶, B. Martin dit Latour¹⁴, H. Martinez¹³⁷, M. Martinez^{12,o}, S. Martin-Haugh¹³¹, V.S. Martoiu^{26a}, A.C. Martyniuk⁷⁸, M. Marx¹³⁹, F. Marzano^{133a}, A. Marzin³⁰, L. Masetti⁸³, T. Mashimo¹⁵⁶, R. Mashinistov⁹⁶, J. Masik⁸⁴, A.L. Maslennikov^{109,c}, I. Massa^{20a,20b}, L. Massa^{20a,20b}, N. Massol⁵, P. Mastrandrea¹⁴⁹, A. Mastroberardino^{37a,37b}, T. Masubuchi¹⁵⁶, P. Mättig¹⁷⁶, J. Mattmann⁸³, J. Maurer^{26a}, S.J. Maxfield⁷⁴, D.A. Maximov^{109,c}, R. Mazini¹⁵², S.M. Mazza^{91a,91b}, L. Mazzaferro^{134a,134b}, G. Mc Goldrick¹⁵⁹, S.P. Mc Kee⁸⁹, A. McCarn⁸⁹, R.L. McCarthy¹⁴⁹, T.G. McCarthy²⁹, N.A. McCubbin¹³¹, K.W. McFarlane^{56,*}, J.A. MCFayden⁷⁸, G. Mchedlidze⁵⁴, S.J. McMahon¹³¹, R.A. McPherson^{170,k}, M. Medinnis⁴², S. Meehan^{146a}, S. Mehlhase¹⁰⁰, A. Mehta⁷⁴, K. Meier^{58a}, C. Meineck¹⁰⁰, B. Meirose⁴¹, C. Melachrinos³¹, B.R. Mellado Garcia^{146c}, F. Meloni¹⁷, A. Mengarelli^{20a,20b}, S. Menke¹⁰¹, E. Meoni¹⁶², K.M. Mercurio⁵⁷, S. Mergelmeyer²¹, N. Meric¹³⁷, P. Mermod⁴⁹, L. Merola^{104a,104b},

C. Meroni^{91a}, F.S. Merritt³¹, H. Merritt¹¹¹, A. Messina^{133a,133b}, J. Metcalfe²⁵, A.S. Mete¹⁶⁴,
 C. Meyer⁸³, C. Meyer¹²², J-P. Meyer¹³⁷, J. Meyer¹⁰⁷, R.P. Middleton¹³¹, S. Miglioranza^{165a,165c},
 L. Mijović²¹, G. Mikenberg¹⁷³, M. Mikestikova¹²⁷, M. Mikuz⁷⁵, M. Milesi⁸⁸, A. Milic³⁰,
 D.W. Miller³¹, C. Mills⁴⁶, A. Milov¹⁷³, D.A. Milstead^{147a,147b}, A.A. Minaenko¹³⁰, Y. Minami¹⁵⁶,
 I.A. Minashvili⁶⁵, A.I. Mincer¹¹⁰, B. Mindur^{38a}, M. Mineev⁶⁵, Y. Ming¹⁷⁴, L.M. Mir¹²,
 G. Mirabelli^{133a}, T. Mitani¹⁷², J. Mitrevski¹⁰⁰, V.A. Mitsou¹⁶⁸, A. Miucci⁴⁹, P.S. Miyagawa¹⁴⁰,
 J.U. Mjörnmark⁸¹, T. Moa^{147a,147b}, K. Mochizuki⁸⁵, S. Mohapatra³⁵, W. Mohr⁴⁸,
 S. Molander^{147a,147b}, R. Moles-Valls¹⁶⁸, K. Mönig⁴², C. Monini⁵⁵, J. Monk³⁶, E. Monnier⁸⁵,
 J. Montejo Berlingen¹², F. Monticelli⁷¹, S. Monzani^{133a,133b}, R.W. Moore³, N. Morange¹¹⁷,
 D. Moreno¹⁶³, M. Moreno Llácer⁵⁴, P. Morettini^{50a}, M. Morgenstern⁴⁴, M. Morii⁵⁷,
 V. Morisbak¹¹⁹, S. Moritz⁸³, A.K. Morley¹⁴⁸, G. Mornacchi³⁰, J.D. Morris⁷⁶, A. Morton⁵³,
 L. Morvaj¹⁰³, M. Mosidze^{51b}, J. Moss¹¹¹, K. Motohashi¹⁵⁸, R. Mount¹⁴⁴, E. Mountricha²⁵,
 S.V. Mouraviev^{96,*}, E.J.W. Moyses⁸⁶, S. Muanza⁸⁵, R.D. Mudd¹⁸, F. Mueller¹⁰¹, J. Mueller¹²⁵,
 K. Mueller²¹, R.S.P. Mueller¹⁰⁰, T. Mueller²⁸, D. Muenstermann⁴⁹, P. Mullen⁵³, Y. Munwes¹⁵⁴,
 J.A. Murillo Quijada¹⁸, W.J. Murray^{171,131}, H. Musheghyan⁵⁴, E. Musto¹⁵³, A.G. Myagkov^{130,aa},
 M. Myska¹²⁸, O. Nackenhorst⁵⁴, J. Nadal⁵⁴, K. Nagai¹²⁰, R. Nagai¹⁵⁸, Y. Nagai⁸⁵, K. Nagano⁶⁶,
 A. Nagarkar¹¹¹, Y. Nagasaka⁵⁹, K. Nagata¹⁶¹, M. Nagel¹⁰¹, E. Nagy⁸⁵, A.M. Nairz³⁰,
 Y. Nakahama³⁰, K. Nakamura⁶⁶, T. Nakamura¹⁵⁶, I. Nakano¹¹², H. Namasivayam⁴¹, G. Nanava²¹,
 R.F. Naranjo Garcia⁴², R. Narayan^{58b}, T. Nattermann²¹, T. Naumann⁴², G. Navarro¹⁶³,
 R. Nayyar⁷, H.A. Neal⁸⁹, P.Yu. Nechaeva⁹⁶, T.J. Neep⁸⁴, P.D. Nef¹⁴⁴, A. Negri^{121a,121b},
 M. Negrini^{20a}, S. Nektarijevic¹⁰⁶, C. Nellist¹¹⁷, A. Nelson¹⁶⁴, S. Nemecek¹²⁷, P. Nemethy¹¹⁰,
 A.A. Nepomuceno^{24a}, M. Nessi^{30,ab}, M.S. Neubauer¹⁶⁶, M. Neumann¹⁷⁶, R.M. Neves¹¹⁰,
 P. Nevski²⁵, P.R. Newman¹⁸, D.H. Nguyen⁶, R.B. Nickerson¹²⁰, R. Nicolaidou¹³⁷,
 B. Nicquevert³⁰, J. Nielsen¹³⁸, N. Nikiforou³⁵, A. Nikiforov¹⁶, V. Nikolaenko^{130,aa},
 I. Nikolic-Audit⁸⁰, K. Nikolopoulos¹⁸, J.K. Nilsen¹¹⁹, P. Nilsson²⁵, Y. Ninomiya¹⁵⁶, A. Nisati^{133a},
 R. Nisius¹⁰¹, T. Nobe¹⁵⁸, M. Nomachi¹¹⁸, I. Nomidis²⁹, T. Nooney⁷⁶, S. Norberg¹¹³,
 M. Nordberg³⁰, O. Novgorodova⁴⁴, S. Nowak¹⁰¹, M. Nozaki⁶⁶, L. Nozka¹¹⁵, K. Ntekas¹⁰,
 G. Nunes Hanninger⁸⁸, T. Nunnemann¹⁰⁰, E. Nurse⁷⁸, F. Nuti⁸⁸, B.J. O'Brien⁴⁶, F. O'grady⁷,
 D.C. O'Neil¹⁴³, V. O'Shea⁵³, F.G. Oakham^{29,d}, H. Oberlack¹⁰¹, T. Obermann²¹, J. Ocariz⁸⁰,
 A. Ochi⁶⁷, I. Ochoa⁷⁸, S. Oda⁷⁰, S. Odaka⁶⁶, H. Ogren⁶¹, A. Oh⁸⁴, S.H. Oh⁴⁵, C.C. Ohm¹⁵,
 H. Ohman¹⁶⁷, H. Oide³⁰, W. Okamura¹¹⁸, H. Okawa¹⁶¹, Y. Okumura³¹, T. Okuyama¹⁵⁶,
 A. Olariu^{26a}, S.A. Olivares Pino⁴⁶, D. Oliveira Damazio²⁵, E. Oliver Garcia¹⁶⁸, A. Olszewski³⁹,
 J. Olszowska³⁹, A. Onofre^{126a,126e}, P.U.E. Onyisi^{31,q}, C.J. Oram^{160a}, M.J. Oreglia³¹, Y. Oren¹⁵⁴,
 D. Orestano^{135a,135b}, N. Orlando¹⁵⁵, C. Oropeza Barrera⁵³, R.S. Orr¹⁵⁹, B. Osculati^{50a,50b},
 R. Ospanov⁸⁴, G. Otero y Garzon²⁷, H. Otono⁷⁰, M. Ouchrif^{136d}, E.A. Ouellette¹⁷⁰,
 F. Ould-Saada¹¹⁹, A. Ouraou¹³⁷, K.P. Oussoren¹⁰⁷, Q. Ouyang^{33a}, A. Ovcharova¹⁵, M. Owen⁵³,
 R.E. Owen¹⁸, V.E. Ozcan^{19a}, N. Ozturk⁸, K. Pachal¹²⁰, A. Pacheco Pages¹², C. Padilla Aranda¹²,
 M. Pagáčová⁴⁸, S. Pagan Griso¹⁵, E. Paganis¹⁴⁰, C. Pahl¹⁰¹, F. Paige²⁵, P. Pais⁸⁶, K. Pajchel¹¹⁹,
 G. Palacino^{160b}, S. Palestini³⁰, M. Palka^{38b}, D. Pallin³⁴, A. Palma^{126a,126b}, Y.B. Pan¹⁷⁴,
 E. Panagiotopoulou¹⁰, C.E. Pandini⁸⁰, J.G. Panduro Vazquez⁷⁷, P. Pani^{147a,147b}, S. Panitkin²⁵,
 D. Pantea^{26a}, L. Paolozzi^{134a,134b}, Th.D. Papadopoulou¹⁰, K. Papageorgiou¹⁵⁵, A. Paramonov⁶,
 D. Paredes Hernandez¹⁵⁵, M.A. Parker²⁸, K.A. Parker¹⁴⁰, F. Parodi^{50a,50b}, J.A. Parsons³⁵,
 U. Parzefall⁴⁸, E. Pasqualucci^{133a}, S. Passaggio^{50a}, F. Pastore^{135a,135b,*}, Fr. Pastore⁷⁷,
 G. Pásztor²⁹, S. Patariaia¹⁷⁶, N.D. Patel¹⁵¹, J.R. Pater⁸⁴, T. Pauly³⁰, J. Pearce¹⁷⁰, B. Pearson¹¹³,
 L.E. Pedersen³⁶, M. Pedersen¹¹⁹, S. Pedraza Lopez¹⁶⁸, R. Pedro^{126a,126b}, S.V. Peleganchuk^{109,c},
 D. Pelikan¹⁶⁷, H. Peng^{33b}, B. Penning³¹, J. Penwell⁶¹, D.V. Perepelitsa²⁵, E. Perez Codina^{160a},
 M.T. Pérez García-Estañ¹⁶⁸, L. Perini^{91a,91b}, H. Pernegger³⁰, S. Perrella^{104a,104b}, R. Peschke⁴²,
 V.D. Peshekhonov⁶⁵, K. Peters³⁰, R.F.Y. Peters⁸⁴, B.A. Petersen³⁰, T.C. Petersen³⁶, E. Petit⁴²,

A. Petridis^{147a,147b}, C. Petridou¹⁵⁵, E. Petrolo^{133a}, F. Petrucci^{135a,135b}, N.E. Pettersson¹⁵⁸,
 R. Pezoa^{32b}, P.W. Phillips¹³¹, G. Piacquadio¹⁴⁴, E. Pianori¹⁷¹, A. Picazio⁴⁹, E. Piccaro⁷⁶,
 M. Piccinini^{20a,20b}, M.A. Pickering¹²⁰, R. Piegai²⁷, D.T. Pignotti¹¹¹, J.E. Pilcher³¹,
 A.D. Pilkington⁷⁸, J. Pina^{126a,126b,126d}, M. Pinamonti^{165a,165c,ac}, J.L. Pinfeld³, A. Pingel³⁶,
 B. Pinto^{126a}, S. Pires⁸⁰, M. Pitt¹⁷³, C. Pizio^{91a,91b}, L. Plazak^{145a}, M.-A. Pleier²⁵, V. Pleskot¹²⁹,
 E. Plotnikova⁶⁵, P. Plucinski^{147a,147b}, D. Pluth⁶⁴, R. Poettgen⁸³, L. Poggioli¹¹⁷, D. Pohl²¹,
 G. Polesello^{121a}, A. Policicchio^{37a,37b}, R. Polifka¹⁵⁹, A. Polini^{20a}, C.S. Pollard⁵³,
 V. Polychronakos²⁵, K. Pommès³⁰, L. Pontecorvo^{133a}, B.G. Pope⁹⁰, G.A. Popeneciu^{26b},
 D.S. Popovic¹³, A. Poppleton³⁰, S. Pospisil¹²⁸, K. Potamianos¹⁵, I.N. Potrap⁶⁵, C.J. Potter¹⁵⁰,
 C.T. Potter¹¹⁶, G. Poulard³⁰, J. Poveda³⁰, V. Pozdnyakov⁶⁵, P. Pralavorio⁸⁵, A. Pranko¹⁵,
 S. Prasad³⁰, S. Prell⁶⁴, D. Price⁸⁴, J. Price⁷⁴, L.E. Price⁶, M. Primavera^{73a}, S. Prince⁸⁷,
 M. Proissl⁴⁶, K. Prokofiev^{60c}, F. Prokoshin^{32b}, E. Protopapadaki¹³⁷, S. Protopopescu²⁵,
 J. Proudfoot⁶, M. Przybycien^{38a}, E. Ptacek¹¹⁶, D. Puddu^{135a,135b}, E. Pueschel⁸⁶, D. Pudlon¹⁴⁹,
 M. Purohit^{25,ad}, P. Puza¹¹⁷, J. Qian⁸⁹, G. Qin⁵³, Y. Qin⁸⁴, A. Quadt⁵⁴, D.R. Quarrie¹⁵,
 W.B. Quayle^{165a,165b}, M. Queitsch-Maitland⁸⁴, D. Quilty⁵³, A. Qureshi^{160b}, S. Raddum¹¹⁹,
 V. Radeka²⁵, V. Radescu⁴², S.K. Radhakrishnan¹⁴⁹, P. Radloff¹¹⁶, P. Rados⁸⁸, F. Ragusa^{91a,91b},
 G. Rahal¹⁷⁹, S. Rajagopalan²⁵, M. Rammensee³⁰, C. Rangel-Smith¹⁶⁷, F. Rauscher¹⁰⁰, S. Rave⁸³,
 T.C. Rave⁴⁸, T. Ravenscroft⁵³, M. Raymond³⁰, A.L. Read¹¹⁹, N.P. Readioff⁷⁴,
 D.M. Rebuzzi^{121a,121b}, A. Redelbach¹⁷⁵, G. Redlinger²⁵, R. Reece¹³⁸, K. Reeves⁴¹, L. Rehnisch¹⁶,
 H. Reisin²⁷, M. Relich¹⁶⁴, C. Rembser³⁰, H. Ren^{33a}, A. Renaud¹¹⁷, M. Rescigno^{133a},
 S. Resconi^{91a}, O.L. Rezanova^{109,c}, P. Reznicek¹²⁹, R. Rezvani⁹⁵, R. Richter¹⁰¹, S. Richter⁷⁸,
 E. Richter-Was^{38b}, M. Ridel⁸⁰, P. Rieck¹⁶, C.J. Riegel¹⁷⁶, J. Rieger⁵⁴, M. Rijssenbeek¹⁴⁹,
 A. Rimoldi^{121a,121b}, L. Rinaldi^{20a}, B. Ristić⁴⁹, E. Ritsch⁶², I. Riu¹², F. Rizatdinova¹¹⁴, E. Rizvi⁷⁶,
 S.H. Robertson^{87,k}, A. Robichaud-Veronneau⁸⁷, D. Robinson²⁸, J.E.M. Robinson⁸⁴, A. Robson⁵³,
 C. Roda^{124a,124b}, L. Rodrigues³⁰, S. Roe³⁰, O. Røhne¹¹⁹, S. Rolli¹⁶², A. Romaniouk⁹⁸,
 M. Romano^{20a,20b}, S.M. Romano Saez³⁴, E. Romero Adam¹⁶⁸, N. Rompotis¹³⁹, M. Ronzani⁴⁸,
 L. Roos⁸⁰, E. Ros¹⁶⁸, S. Rosati^{133a}, K. Rosbach⁴⁸, P. Rose¹³⁸, P.L. Rosendahl¹⁴, O. Rosenthal¹⁴²,
 V. Rossetti^{147a,147b}, E. Rossi^{104a,104b}, L.P. Rossi^{50a}, R. Rosten¹³⁹, M. Rotaru^{26a}, I. Roth¹⁷³,
 J. Rothberg¹³⁹, D. Rousseau¹¹⁷, C.R. Royon¹³⁷, A. Rozanov⁸⁵, Y. Rozen¹⁵³, X. Ruan^{146c},
 F. Rubbo¹⁴⁴, I. Rubinskiy⁴², V.I. Rud⁹⁹, C. Rudolph⁴⁴, M.S. Rudolph¹⁵⁹, F. Rühr⁴⁸,
 A. Ruiz-Martinez³⁰, Z. Rurikova⁴⁸, N.A. Rusakovich⁶⁵, A. Ruschke¹⁰⁰, H.L. Russell¹³⁹,
 J.P. Rutherford⁷, N. Ruthmann⁴⁸, Y.F. Ryabov¹²³, M. Rybar¹²⁹, G. Rybkin¹¹⁷, N.C. Ryder¹²⁰,
 A.F. Saavedra¹⁵¹, G. Sabato¹⁰⁷, S. Sacerdoti²⁷, A. Saddique³, H.F.W. Sadrozinski¹³⁸,
 R. Sadykov⁶⁵, F. Safai Tehrani^{133a}, M. Saimpert¹³⁷, H. Sakamoto¹⁵⁶, Y. Sakurai¹⁷²,
 G. Salamanna^{135a,135b}, A. Salamon^{134a}, M. Saleem¹¹³, D. Salek¹⁰⁷, P.H. Sales De Bruin¹³⁹,
 D. Salihagic¹⁰¹, A. Salnikov¹⁴⁴, J. Salt¹⁶⁸, D. Salvatore^{37a,37b}, F. Salvatore¹⁵⁰, A. Salvucci¹⁰⁶,
 A. Salzburger³⁰, D. Sampsonidis¹⁵⁵, A. Sanchez^{104a,104b}, J. Sánchez¹⁶⁸, V. Sanchez Martinez¹⁶⁸,
 H. Sandaker¹⁴, R.L. Sandbach⁷⁶, H.G. Sander⁸³, M.P. Sanders¹⁰⁰, M. Sandhoff¹⁷⁶, C. Sandoval¹⁶³,
 R. Sandstroem¹⁰¹, D.P.C. Sankey¹³¹, M. Sannino^{50a,50b}, A. Sansoni⁴⁷, C. Santoni³⁴,
 R. Santonico^{134a,134b}, H. Santos^{126a}, I. Santoyo Castillo¹⁵⁰, K. Sapp¹²⁵, A. Saprnov⁶⁵,
 J.G. Saraiva^{126a,126d}, B. Sarrazin²¹, O. Sasaki⁶⁶, Y. Sasaki¹⁵⁶, K. Sato¹⁶¹, G. Sauvage^{5,*},
 E. Sauvan⁵, G. Savage⁷⁷, P. Savard^{159,d}, C. Sawyer¹²⁰, L. Sawyer^{79,n}, J. Saxon³¹, C. Sbarra^{20a},
 A. Sbrizzi^{20a,20b}, T. Scanlon⁷⁸, D.A. Scannicchio¹⁶⁴, M. Scarcella¹⁵¹, V. Scarfone^{37a,37b},
 J. Schaarschmidt¹⁷³, P. Schacht¹⁰¹, D. Schaefer³⁰, R. Schaefer⁴², J. Schaeffer⁸³, S. Schaepe²¹,
 S. Schaezel^{58b}, U. Schäfer⁸³, A.C. Schaffer¹¹⁷, D. Schaile¹⁰⁰, R.D. Schamberger¹⁴⁹, V. Scharf^{58a},
 V.A. Schegelsky¹²³, D. Scheirich¹²⁹, M. Schernau¹⁶⁴, C. Schiavi^{50a,50b}, C. Schillo⁴⁸,
 M. Schioppa^{37a,37b}, S. Schlenker³⁰, E. Schmidt⁴⁸, K. Schmieden³⁰, C. Schmitt⁸³, S. Schmitt^{58b},
 S. Schmitt⁴², B. Schneider^{160a}, Y.J. Schnellbach⁷⁴, U. Schnoor⁴⁴, L. Schoeffel¹³⁷, A. Schoening^{58b},

B.D. Schoenrock⁹⁰, E. Schopf²¹, A.L.S. Schorlemmer⁵⁴, M. Schott⁸³, D. Schouten^{160a},
 J. Schovancova⁸, S. Schramm¹⁵⁹, M. Schreyer¹⁷⁵, C. Schroeder⁸³, N. Schuh⁸³, M.J. Schultens²¹,
 H.-C. Schultz-Coulon^{58a}, H. Schulz¹⁶, M. Schumacher⁴⁸, B.A. Schumm¹³⁸, Ph. Schune¹³⁷,
 C. Schwanenberger⁸⁴, A. Schwartzman¹⁴⁴, T.A. Schwarz⁸⁹, Ph. Schwegler¹⁰¹, Ph. Schwemling¹³⁷,
 R. Schwienhorst⁹⁰, J. Schwindling¹³⁷, T. Schwindt²¹, M. Schwoerer⁵, F.G. Sciacca¹⁷, E. Scifo¹¹⁷,
 G. Sciolla²³, F. Scuri^{124a,124b}, F. Scutti²¹, J. Searcy⁸⁹, G. Sedov⁴², E. Sedykh¹²³, P. Seema²¹,
 S.C. Seidel¹⁰⁵, A. Seiden¹³⁸, F. Seifert¹²⁸, J.M. Seixas^{24a}, G. Sekhniaidze^{104a}, S.J. Sekula⁴⁰,
 K.E. Selbach⁴⁶, D.M. Seliverstov^{123,*}, N. Semprini-Cesari^{20a,20b}, C. Serfon³⁰, L. Serin¹¹⁷,
 L. Serkin⁵⁴, T. Serre⁸⁵, R. Seuster^{160a}, H. Severini¹¹³, T. Sfiligoj⁷⁵, F. Sforza¹⁰¹, A. Sfyrla³⁰,
 E. Shabalina⁵⁴, M. Shamim¹¹⁶, L.Y. Shan^{33a}, R. Shang¹⁶⁶, J.T. Shank²², M. Shapiro¹⁵,
 P.B. Shatalov⁹⁷, K. Shaw^{165a,165b}, A. Shcherbakova^{147a,147b}, C.Y. Shehu¹⁵⁰, P. Sherwood⁷⁸,
 L. Shi^{152,ae}, S. Shimizu⁶⁷, C.O. Shimmin¹⁶⁴, M. Shimojima¹⁰², M. Shiyakova⁶⁵, A. Shmeleva⁹⁶,
 D. Shoaleh Saadi⁹⁵, M.J. Shochet³¹, S. Shojaii^{91a,91b}, S. Shrestha¹¹¹, E. Shulga⁹⁸, M.A. Shupe⁷,
 S. Shushkevich⁴², P. Sicho¹²⁷, O. Sidiropoulou¹⁷⁵, D. Sidorov¹¹⁴, A. Sidoti^{20a,20b}, F. Siegert⁴⁴,
 Dj. Sijacki¹³, J. Silva^{126a,126d}, Y. Silver¹⁵⁴, D. Silverstein¹⁴⁴, S.B. Silverstein^{147a}, V. Simak¹²⁸,
 O. Simard⁵, Lj. Simic¹³, S. Simion¹¹⁷, E. Simioni⁸³, B. Simmons⁷⁸, D. Simon³⁴,
 R. Simoniello^{91a,91b}, P. Sinervo¹⁵⁹, N.B. Sinev¹¹⁶, G. Siragusa¹⁷⁵, A.N. Sisakyan^{65,*},
 S.Yu. Sivoklokov⁹⁹, J. Sjölín^{147a,147b}, T.B. Sjursen¹⁴, M.B. Skinner⁷², H.P. Skottowe⁵⁷,
 P. Skubic¹¹³, M. Slater¹⁸, T. Slavicek¹²⁸, M. Slawinska¹⁰⁷, K. Sliwa¹⁶², V. Smakhtin¹⁷³,
 B.H. Smart⁴⁶, L. Smestad¹⁴, S.Yu. Smirnov⁹⁸, Y. Smirnov⁹⁸, L.N. Smirnova^{99,af}, O. Smirnova⁸¹,
 M.N.K. Smith³⁵, M. Smizanska⁷², K. Smolek¹²⁸, A.A. Snesarev⁹⁶, G. Snidero⁷⁶, S. Snyder²⁵,
 R. Sobie^{170,k}, F. Socher⁴⁴, A. Soffer¹⁵⁴, D.A. Soh^{152,ae}, C.A. Solans³⁰, M. Solar¹²⁸, J. Solc¹²⁸,
 E.Yu. Soldatov⁹⁸, U. Soldevila¹⁶⁸, A.A. Solodkov¹³⁰, A. Soloshenko⁶⁵, O.V. Solovyanov¹³⁰,
 V. Solovyev¹²³, P. Sommer⁴⁸, H.Y. Song^{33b}, N. Soni¹, A. Sood¹⁵, A. Sopczak¹²⁸, B. Sopko¹²⁸,
 V. Sopko¹²⁸, V. Sorin¹², D. Sosa^{58b}, M. Sosebee⁸, C.L. Sotiropoulou¹⁵⁵, R. Soualah^{165a,165c},
 P. Soueid⁹⁵, A.M. Soukharev^{109,c}, D. South⁴², S. Spagnolo^{73a,73b}, M. Spalla^{124a,124b}, F. Spanò⁷⁷,
 W.R. Spearman⁵⁷, F. Spettel¹⁰¹, R. Spighi^{20a}, G. Spigo³⁰, L.A. Spiller⁸⁸, M. Spousta¹²⁹,
 T. Spreitzer¹⁵⁹, R.D. St. Denis^{53,*}, S. Staerz⁴⁴, J. Stahlman¹²², R. Stamen^{58a}, S. Stamm¹⁶,
 E. Stanecka³⁹, C. Stanescu^{135a}, M. Stanescu-Bellu⁴², M.M. Stanitzki⁴², S. Stapnes¹¹⁹,
 E.A. Starchenko¹³⁰, J. Stark⁵⁵, P. Staroba¹²⁷, P. Starovoitov⁴², R. Staszewski³⁹, P. Stavina^{145a,*},
 P. Steinberg²⁵, B. Stelzer¹⁴³, H.J. Stelzer³⁰, O. Stelzer-Chilton^{160a}, H. Stenzel⁵², S. Stern¹⁰¹,
 G.A. Stewart⁵³, J.A. Stillings²¹, M.C. Stockton⁸⁷, M. Stoebe⁸⁷, G. Stoicea^{26a}, P. Stolte⁵⁴,
 S. Stonjek¹⁰¹, A.R. Stradling⁸, A. Straessner⁴⁴, M.E. Stramaglia¹⁷, J. Strandberg¹⁴⁸,
 S. Strandberg^{147a,147b}, A. Strandlie¹¹⁹, E. Strauss¹⁴⁴, M. Strauss¹¹³, P. Strizeneč^{145b},
 R. Ströhmer¹⁷⁵, D.M. Strom¹¹⁶, R. Stroynowski⁴⁰, A. Strubig¹⁰⁶, S.A. Stucci¹⁷, B. Stugu¹⁴,
 N.A. Styles⁴², D. Su¹⁴⁴, J. Su¹²⁵, R. Subramaniam⁷⁹, A. Succurro¹², Y. Sugaya¹¹⁸, C. Suhr¹⁰⁸,
 M. Suk¹²⁸, V.V. Sulin⁹⁶, S. Sultansoy^{4d}, T. Sumida⁶⁸, S. Sun⁵⁷, X. Sun^{33a}, J.E. Sundermann⁴⁸,
 K. Suruliz¹⁵⁰, G. Susinno^{37a,37b}, M.R. Sutton¹⁵⁰, Y. Suzuki⁶⁶, M. Svatos¹²⁷, S. Swedish¹⁶⁹,
 M. Swiatlowski¹⁴⁴, I. Sykora^{145a}, T. Sykora¹²⁹, D. Ta⁹⁰, C. Taccini^{135a,135b}, K. Tackmann⁴²,
 J. Taenzer¹⁵⁹, A. Taffard¹⁶⁴, R. Tafirout^{160a}, N. Taiblum¹⁵⁴, H. Takai²⁵, R. Takashima⁶⁹,
 H. Takeda⁶⁷, T. Takeshita¹⁴¹, Y. Takubo⁶⁶, M. Talby⁸⁵, A.A. Talyshev^{109,c}, J.Y.C. Tam¹⁷⁵,
 K.G. Tan⁸⁸, J. Tanaka¹⁵⁶, R. Tanaka¹¹⁷, S. Tanaka¹³², S. Tanaka⁶⁶, A.J. Tanasijczuk¹⁴³,
 B.B. Tannenwald¹¹¹, N. Tannoury²¹, S. Tapprogge⁸³, S. Tarem¹⁵³, F. Tarrade²⁹,
 G.F. Tartarelli^{91a}, P. Tas¹²⁹, M. Tasevsky¹²⁷, T. Tashiro⁶⁸, E. Tassi^{37a,37b},
 A. Tavares Delgado^{126a,126b}, Y. Tayalati^{136d}, F.E. Taylor⁹⁴, G.N. Taylor⁸⁸, W. Taylor^{160b},
 F.A. Teischinger³⁰, M. Teixeira Dias Castanheira⁷⁶, P. Teixeira-Dias⁷⁷, K.K. Temming⁴⁸,
 H. Ten Kate³⁰, P.K. Teng¹⁵², J.J. Teoh¹¹⁸, F. Tepel¹⁷⁶, S. Terada⁶⁶, K. Terashi¹⁵⁶, J. Terron⁸²,
 S. Terzo¹⁰¹, M. Testa⁴⁷, R.J. Teuscher^{159,k}, J. Therhaag²¹, T. Theveneaux-Pelzer³⁴,

J.P. Thomas¹⁸, J. Thomas-Wilsker⁷⁷, E.N. Thompson³⁵, P.D. Thompson¹⁸, R.J. Thompson⁸⁴, A.S. Thompson⁵³, L.A. Thomsen³⁶, E. Thomson¹²², M. Thomson²⁸, R.P. Thun^{89,*}, F. Tian³⁵, M.J. Tibbetts¹⁵, R.E. Ticse Torres⁸⁵, V.O. Tikhomirov^{96,ag}, Yu.A. Tikhonov^{109,c}, S. Timoshenko⁹⁸, E. Tiouchichine⁸⁵, P. Tipton¹⁷⁷, S. Tisserant⁸⁵, T. Todorov^{5,*}, S. Todorova-Nova¹²⁹, J. Tojo⁷⁰, S. Tokár^{145a}, K. Tokushuku⁶⁶, K. Tollefson⁹⁰, E. Tolley⁵⁷, L. Tomlinson⁸⁴, M. Tomoto¹⁰³, L. Tompkins^{144,ah}, K. Toms¹⁰⁵, E. Torrence¹¹⁶, H. Torres¹⁴³, E. Torró Pastor¹⁶⁸, J. Toth^{85,ai}, F. Touchard⁸⁵, D.R. Tovey¹⁴⁰, H.L. Tran¹¹⁷, T. Trefzger¹⁷⁵, L. Tremblet³⁰, A. Tricoli³⁰, I.M. Trigger^{160a}, S. Trincaz-Duvoid⁸⁰, M.F. Tripiana¹², W. Trischuk¹⁵⁹, B. Trocme⁵⁵, C. Troncon^{91a}, M. Trotter-McDonald¹⁵, M. Trovatelli^{135a,135b}, P. True⁹⁰, M. Trzebinski³⁹, A. Trzupek³⁹, C. Tsarouchas³⁰, J.C-L. Tseng¹²⁰, P.V. Tsiareshka⁹², D. Tsionou¹⁵⁵, G. Tsipolitis¹⁰, N. Tsirintanis⁹, S. Tsiskaridze¹², V. Tsiskaridze⁴⁸, E.G. Tskhadadze^{51a}, I.I. Tsukerman⁹⁷, V. Tsulaia¹⁵, S. Tsuno⁶⁶, D. Tsybychev¹⁴⁹, A. Tudorache^{26a}, V. Tudorache^{26a}, A.N. Tuna¹²², S.A. Tuppuri^{20a,20b}, S. Turchikhin^{99,af}, D. Turecek¹²⁸, R. Turra^{91a,91b}, A.J. Turvey⁴⁰, P.M. Tuts³⁵, A. Tykhonov⁴⁹, M. Tylmad^{147a,147b}, M. Tyndel¹³¹, I. Ueda¹⁵⁶, R. Ueno²⁹, M. Ughetto^{147a,147b}, M. Uglan¹⁴, M. Uhlenbrock²¹, F. Ukegawa¹⁶¹, G. Unal³⁰, A. Undrus²⁵, G. Unel¹⁶⁴, F.C. Ungaro⁴⁸, Y. Unno⁶⁶, C. Unverdorben¹⁰⁰, J. Urban^{145b}, P. Urquijo⁸⁸, P. Urrejola⁸³, G. Usai⁸, A. Usanova⁶², L. Vacavant⁸⁵, V. Vacek¹²⁸, B. Vachon⁸⁷, C. Valderanis⁸³, N. Valencic¹⁰⁷, S. Valentinetti^{20a,20b}, A. Valero¹⁶⁸, L. Valery¹², S. Valkar¹²⁹, E. Valladolid Gallego¹⁶⁸, S. Vallecorsa⁴⁹, J.A. Valls Ferrer¹⁶⁸, W. Van Den Wollenberg¹⁰⁷, P.C. Van Der Deijl¹⁰⁷, R. van der Geer¹⁰⁷, H. van der Graaf¹⁰⁷, R. Van Der Leeuw¹⁰⁷, N. van Eldik¹⁵³, P. van Gemmeren⁶, J. Van Nieuwkoop¹⁴³, I. van Vulpen¹⁰⁷, M.C. van Woerden³⁰, M. Vanadia^{133a,133b}, W. Vandelli³⁰, R. Vanguri¹²², A. Vaniachine⁶, F. Vannucci⁸⁰, G. Vardanyan¹⁷⁸, R. Vari^{133a}, E.W. Varnes⁷, T. Varol⁴⁰, D. Varouchas⁸⁰, A. Vartapetian⁸, K.E. Varvell¹⁵¹, F. Vazeille³⁴, T. Vazquez Schroeder⁵⁴, J. Veatch⁷, F. Veloso^{126a,126c}, T. Velz²¹, S. Veneziano^{133a}, A. Ventura^{73a,73b}, D. Ventura⁸⁶, M. Venturi¹⁷⁰, N. Venturi¹⁵⁹, A. Venturini²³, V. Vercesi^{121a}, M. Verducci^{133a,133b}, W. Verkerke¹⁰⁷, J.C. Vermeulen¹⁰⁷, A. Vest⁴⁴, M.C. Vetterli^{143,d}, O. Viazlo⁸¹, I. Vichou¹⁶⁶, T. Vickey^{146c,aj}, O.E. Vickey Boeriu^{146c}, G.H.A. Viehhauser¹²⁰, S. Viel¹⁵, R. Vigne³⁰, M. Villa^{20a,20b}, M. Villaplana Perez^{91a,91b}, E. Vilucchi⁴⁷, M.G. Vincker²⁹, V.B. Vinogradov⁶⁵, I. Vivarelli¹⁵⁰, F. Vives Vaque³, S. Vlachos¹⁰, D. Vladoiu¹⁰⁰, M. Vlasak¹²⁸, M. Vogel^{32a}, P. Vokac¹²⁸, G. Volpi^{124a,124b}, M. Volpi⁸⁸, H. von der Schmitt¹⁰¹, H. von Radziewski⁴⁸, E. von Toerne²¹, V. Vorobel¹²⁹, K. Vorobev⁹⁸, M. Vos¹⁶⁸, R. Voss³⁰, J.H. Vosseveld⁷⁴, N. Vranjes¹³, M. Vranjes Milosavljevic¹³, V. Vrba¹²⁷, M. Vreeswijk¹⁰⁷, R. Vuillermet³⁰, I. Vukotic³¹, Z. Vykydal¹²⁸, P. Wagner²¹, W. Wagner¹⁷⁶, H. Wahlberg⁷¹, S. Wahrenmund⁴⁴, J. Wakabayashi¹⁰³, J. Walder⁷², R. Walker¹⁰⁰, W. Walkowiak¹⁴², C. Wang^{33c}, F. Wang¹⁷⁴, H. Wang¹⁵, H. Wang⁴⁰, J. Wang⁴², J. Wang^{33a}, K. Wang⁸⁷, R. Wang⁶, S.M. Wang¹⁵², T. Wang²¹, X. Wang¹⁷⁷, C. Wanotayaroj¹¹⁶, A. Warburton⁸⁷, C.P. Ward²⁸, D.R. Wardrope⁷⁸, M. Warsinsky⁴⁸, A. Washbrook⁴⁶, C. Wasicki⁴², P.M. Watkins¹⁸, A.T. Watson¹⁸, I.J. Watson¹⁵¹, M.F. Watson¹⁸, G. Watts¹³⁹, S. Watts⁸⁴, B.M. Waugh⁷⁸, S. Webb⁸⁴, M.S. Weber¹⁷, S.W. Weber¹⁷⁵, J.S. Webster³¹, A.R. Weidberg¹²⁰, B. Weinert⁶¹, J. Weingarten⁵⁴, C. Weiser⁴⁸, H. Weits¹⁰⁷, P.S. Wells³⁰, T. Wenaus²⁵, D. Wendland¹⁶, T. Wengler³⁰, S. Wenig³⁰, N. Wermes²¹, M. Werner⁴⁸, P. Werner³⁰, M. Wessels^{58a}, J. Wetter¹⁶², K. Whalen²⁹, A.M. Wharton⁷², A. White⁸, M.J. White¹, R. White^{32b}, S. White^{124a,124b}, D. Whiteson¹⁶⁴, D. Wicke¹⁷⁶, F.J. Wickens¹³¹, W. Wiedenmann¹⁷⁴, M. Wielers¹³¹, P. Wienemann²¹, C. Wiglesworth³⁶, L.A.M. Wiik-Fuchs²¹, A. Wildauer¹⁰¹, H.G. Wilkens³⁰, H.H. Williams¹²², S. Williams¹⁰⁷, C. Willis⁹⁰, S. Willocq⁸⁶, A. Wilson⁸⁹, J.A. Wilson¹⁸, I. Wingerter-Seez⁵, F. Winklmeier¹¹⁶, B.T. Winter²¹, M. Wittgen¹⁴⁴, J. Wittkowski¹⁰⁰, S.J. Wollstadt⁸³, M.W. Wolter³⁹, H. Wolters^{126a,126c}, B.K. Wosiek³⁹, J. Wotschack³⁰, M.J. Woudstra⁸⁴, K.W. Wozniak³⁹, M. Wu⁵⁵,

M. Wu³¹, S.L. Wu¹⁷⁴, X. Wu⁴⁹, Y. Wu⁸⁹, T.R. Wyatt⁸⁴, B.M. Wynne⁴⁶, S. Xella³⁶, D. Xu^{33a}, L. Xu^{33b,ak}, B. Yabsley¹⁵¹, S. Yacoob^{146b,al}, R. Yakabe⁶⁷, M. Yamada⁶⁶, Y. Yamaguchi¹¹⁸, A. Yamamoto⁶⁶, S. Yamamoto¹⁵⁶, T. Yamanaka¹⁵⁶, K. Yamauchi¹⁰³, Y. Yamazaki⁶⁷, Z. Yan²², H. Yang^{33e}, H. Yang¹⁷⁴, Y. Yang¹⁵², L. Yao^{33a}, W.-M. Yao¹⁵, Y. Yasu⁶⁶, E. Yatsenko⁴², K.H. Yau Wong²¹, J. Ye⁴⁰, S. Ye²⁵, I. Yeletsikh⁶⁵, A.L. Yen⁵⁷, E. Yildirim⁴², K. Yorita¹⁷², R. Yoshida⁶, K. Yoshihara¹²², C. Young¹⁴⁴, C.J.S. Young³⁰, S. Youssef²², D.R. Yu¹⁵, J. Yu⁸, J.M. Yu⁸⁹, J. Yu¹¹⁴, L. Yuan⁶⁷, A. Yurkewicz¹⁰⁸, I. Yusuff^{28,am}, B. Zabinski³⁹, R. Zaidan⁶³, A.M. Zaitsev^{130,aa}, J. Zalieckas¹⁴, A. Zaman¹⁴⁹, S. Zambito²³, L. Zanello^{133a,133b}, D. Zanzi⁸⁸, C. Zeitnitz¹⁷⁶, M. Zeman¹²⁸, A. Zemla^{38a}, K. Zengel²³, O. Zenin¹³⁰, T. Ženiš^{145a}, D. Zerwas¹¹⁷, D. Zhang⁸⁹, F. Zhang¹⁷⁴, J. Zhang⁶, L. Zhang¹⁵², R. Zhang^{33b}, X. Zhang^{33d}, Z. Zhang¹¹⁷, X. Zhao⁴⁰, Y. Zhao^{33d,117}, Z. Zhao^{33b}, A. Zhemchugov⁶⁵, J. Zhong¹²⁰, B. Zhou⁸⁹, C. Zhou⁴⁵, L. Zhou³⁵, L. Zhou⁴⁰, N. Zhou¹⁶⁴, C.G. Zhu^{33d}, H. Zhu^{33a}, J. Zhu⁸⁹, Y. Zhu^{33b}, X. Zhuang^{33a}, K. Zhukov⁹⁶, A. Zibell¹⁷⁵, D. Zieminska⁶¹, N.I. Zimine⁶⁵, C. Zimmermann⁸³, R. Zimmermann²¹, S. Zimmermann⁴⁸, Z. Zinonos⁵⁴, M. Zinser⁸³, M. Ziolkowski¹⁴², L. Živković¹³, G. Zobernig¹⁷⁴, A. Zoccolì^{20a,20b}, M. zur Nedden¹⁶, G. Zurzolo^{104a,104b} and L. Zwalinski³⁰.

¹ *Department of Physics, University of Adelaide, Adelaide, Australia*

² *Physics Department, SUNY Albany, Albany NY, United States of America*

³ *Department of Physics, University of Alberta, Edmonton AB, Canada*

⁴ ^(a) *Department of Physics, Ankara University, Ankara;* ^(c) *Istanbul Aydin University, Istanbul;* ^(d) *Division of Physics, TOBB University of Economics and Technology, Ankara, Turkey*

⁵ *LAPP, CNRS/IN2P3 and Université Savoie Mont Blanc, Annecy-le-Vieux, France*

⁶ *High Energy Physics Division, Argonne National Laboratory, Argonne IL, United States of America*

⁷ *Department of Physics, University of Arizona, Tucson AZ, United States of America*

⁸ *Department of Physics, The University of Texas at Arlington, Arlington TX, United States of America*

⁹ *Physics Department, University of Athens, Athens, Greece*

¹⁰ *Physics Department, National Technical University of Athens, Zografou, Greece*

¹¹ *Institute of Physics, Azerbaijan Academy of Sciences, Baku, Azerbaijan*

¹² *Institut de Física d'Altes Energies and Departament de Física de la Universitat Autònoma de Barcelona, Barcelona, Spain*

¹³ *Institute of Physics, University of Belgrade, Belgrade, Serbia*

¹⁴ *Department for Physics and Technology, University of Bergen, Bergen, Norway*

¹⁵ *Physics Division, Lawrence Berkeley National Laboratory and University of California, Berkeley CA, United States of America*

¹⁶ *Department of Physics, Humboldt University, Berlin, Germany*

¹⁷ *Albert Einstein Center for Fundamental Physics and Laboratory for High Energy Physics, University of Bern, Bern, Switzerland*

¹⁸ *School of Physics and Astronomy, University of Birmingham, Birmingham, United Kingdom*

¹⁹ ^(a) *Department of Physics, Bogazici University, Istanbul;* ^(b) *Department of Physics, Dogus University, Istanbul;* ^(c) *Department of Physics Engineering, Gaziantep University, Gaziantep, Turkey*

²⁰ ^(a) *INFN Sezione di Bologna;* ^(b) *Dipartimento di Fisica e Astronomia, Università di Bologna, Bologna, Italy*

²¹ *Physikalisches Institut, University of Bonn, Bonn, Germany*

²² *Department of Physics, Boston University, Boston MA, United States of America*

²³ *Department of Physics, Brandeis University, Waltham MA, United States of America*

²⁴ ^(a) *Universidade Federal do Rio De Janeiro COPPE/EE/IF, Rio de Janeiro;* ^(b) *Electrical Circuits Department, Federal University of Juiz de Fora (UFJF), Juiz de Fora;* ^(c) *Federal University of Sao Joao del Rei (UFSJ), Sao Joao del Rei;* ^(d) *Instituto de Física, Universidade de Sao Paulo, Sao Paulo, Brazil*

- 25 *Physics Department, Brookhaven National Laboratory, Upton NY, United States of America*
- 26 ^(a) *National Institute of Physics and Nuclear Engineering, Bucharest;* ^(b) *National Institute for Research and Development of Isotopic and Molecular Technologies, Physics Department, Cluj Napoca;* ^(c) *University Politehnica Bucharest, Bucharest;* ^(d) *West University in Timisoara, Timisoara, Romania*
- 27 *Departamento de Física, Universidad de Buenos Aires, Buenos Aires, Argentina*
- 28 *Cavendish Laboratory, University of Cambridge, Cambridge, United Kingdom*
- 29 *Department of Physics, Carleton University, Ottawa ON, Canada*
- 30 *CERN, Geneva, Switzerland*
- 31 *Enrico Fermi Institute, University of Chicago, Chicago IL, United States of America*
- 32 ^(a) *Departamento de Física, Pontificia Universidad Católica de Chile, Santiago;* ^(b) *Departamento de Física, Universidad Técnica Federico Santa María, Valparaíso, Chile*
- 33 ^(a) *Institute of High Energy Physics, Chinese Academy of Sciences, Beijing;* ^(b) *Department of Modern Physics, University of Science and Technology of China, Anhui;* ^(c) *Department of Physics, Nanjing University, Jiangsu;* ^(d) *School of Physics, Shandong University, Shandong;* ^(e) *Department of Physics and Astronomy, Shanghai Key Laboratory for Particle Physics and Cosmology, Shanghai Jiao Tong University, Shanghai;* ^(f) *Physics Department, Tsinghua University, Beijing 100084, China*
- 34 *Laboratoire de Physique Corpusculaire, Clermont Université and Université Blaise Pascal and CNRS/IN2P3, Clermont-Ferrand, France*
- 35 *Nevis Laboratory, Columbia University, Irvington NY, United States of America*
- 36 *Niels Bohr Institute, University of Copenhagen, Kobenhavn, Denmark*
- 37 ^(a) *INFN Gruppo Collegato di Cosenza, Laboratori Nazionali di Frascati;* ^(b) *Dipartimento di Fisica, Università della Calabria, Rende, Italy*
- 38 ^(a) *AGH University of Science and Technology, Faculty of Physics and Applied Computer Science, Krakow;* ^(b) *Marian Smoluchowski Institute of Physics, Jagiellonian University, Krakow, Poland*
- 39 *Institute of Nuclear Physics Polish Academy of Sciences, Krakow, Poland*
- 40 *Physics Department, Southern Methodist University, Dallas TX, United States of America*
- 41 *Physics Department, University of Texas at Dallas, Richardson TX, United States of America*
- 42 *DESY, Hamburg and Zeuthen, Germany*
- 43 *Institut für Experimentelle Physik IV, Technische Universität Dortmund, Dortmund, Germany*
- 44 *Institut für Kern- und Teilchenphysik, Technische Universität Dresden, Dresden, Germany*
- 45 *Department of Physics, Duke University, Durham NC, United States of America*
- 46 *SUPA - School of Physics and Astronomy, University of Edinburgh, Edinburgh, United Kingdom*
- 47 *INFN Laboratori Nazionali di Frascati, Frascati, Italy*
- 48 *Fakultät für Mathematik und Physik, Albert-Ludwigs-Universität, Freiburg, Germany*
- 49 *Section de Physique, Université de Genève, Geneva, Switzerland*
- 50 ^(a) *INFN Sezione di Genova;* ^(b) *Dipartimento di Fisica, Università di Genova, Genova, Italy*
- 51 ^(a) *E. Andronikashvili Institute of Physics, Iv. Javakishvili Tbilisi State University, Tbilisi;* ^(b) *High Energy Physics Institute, Tbilisi State University, Tbilisi, Georgia*
- 52 *II Physikalisches Institut, Justus-Liebig-Universität Giessen, Giessen, Germany*
- 53 *SUPA - School of Physics and Astronomy, University of Glasgow, Glasgow, United Kingdom*
- 54 *II Physikalisches Institut, Georg-August-Universität, Göttingen, Germany*
- 55 *Laboratoire de Physique Subatomique et de Cosmologie, Université Grenoble-Alpes, CNRS/IN2P3, Grenoble, France*
- 56 *Department of Physics, Hampton University, Hampton VA, United States of America*
- 57 *Laboratory for Particle Physics and Cosmology, Harvard University, Cambridge MA, United States of America*
- 58 ^(a) *Kirchhoff-Institut für Physik, Ruprecht-Karls-Universität Heidelberg, Heidelberg;* ^(b) *Physikalisches Institut, Ruprecht-Karls-Universität Heidelberg, Heidelberg;* ^(c) *ZITI Institut für technische Informatik, Ruprecht-Karls-Universität Heidelberg, Mannheim, Germany*
- 59 *Faculty of Applied Information Science, Hiroshima Institute of Technology, Hiroshima, Japan*

- 60 ^(a) *Department of Physics, The Chinese University of Hong Kong, Shatin, N.T., Hong Kong;* ^(b)
Department of Physics, The University of Hong Kong, Hong Kong; ^(c) *Department of Physics, The*
61 *Hong Kong University of Science and Technology, Clear Water Bay, Kowloon, Hong Kong, China*
- 62 *Department of Physics, Indiana University, Bloomington IN, United States of America*
- 63 *Institut für Astro- und Teilchenphysik, Leopold-Franzens-Universität, Innsbruck, Austria*
- 64 *University of Iowa, Iowa City IA, United States of America*
- 65 *Department of Physics and Astronomy, Iowa State University, Ames IA, United States of America*
- 66 *Joint Institute for Nuclear Research, JINR Dubna, Dubna, Russia*
- 67 *KEK, High Energy Accelerator Research Organization, Tsukuba, Japan*
- 68 *Graduate School of Science, Kobe University, Kobe, Japan*
- 69 *Faculty of Science, Kyoto University, Kyoto, Japan*
- 70 *Kyoto University of Education, Kyoto, Japan*
- 71 *Department of Physics, Kyushu University, Fukuoka, Japan*
- 72 *Instituto de Física La Plata, Universidad Nacional de La Plata and CONICET, La Plata, Argentina*
- 73 *Physics Department, Lancaster University, Lancaster, United Kingdom*
- 74 ^(a) *INFN Sezione di Lecce;* ^(b) *Dipartimento di Matematica e Fisica, Università del Salento, Lecce,*
Italy
- 75 *Oliver Lodge Laboratory, University of Liverpool, Liverpool, United Kingdom*
- 76 *Department of Physics, Jožef Stefan Institute and University of Ljubljana, Ljubljana, Slovenia*
- 77 *School of Physics and Astronomy, Queen Mary University of London, London, United Kingdom*
- 78 *Department of Physics, Royal Holloway University of London, Surrey, United Kingdom*
- 79 *Department of Physics and Astronomy, University College London, London, United Kingdom*
- 80 *Louisiana Tech University, Ruston LA, United States of America*
- 81 *Laboratoire de Physique Nucléaire et de Hautes Energies, UPMC and Université Paris-Diderot and*
CNRS/IN2P3, Paris, France
- 82 *Fysiska institutionen, Lunds universitet, Lund, Sweden*
- 83 *Departamento de Física Teórica C-15, Universidad Autónoma de Madrid, Madrid, Spain*
- 84 *Institut für Physik, Universität Mainz, Mainz, Germany*
- 85 *School of Physics and Astronomy, University of Manchester, Manchester, United Kingdom*
- 86 *CPPM, Aix-Marseille Université and CNRS/IN2P3, Marseille, France*
- 87 *Department of Physics, University of Massachusetts, Amherst MA, United States of America*
- 88 *Department of Physics, McGill University, Montreal QC, Canada*
- 89 *School of Physics, University of Melbourne, Victoria, Australia*
- 90 *Department of Physics, The University of Michigan, Ann Arbor MI, United States of America*
- 91 *Department of Physics and Astronomy, Michigan State University, East Lansing MI, United States*
of America
- 92 ^(a) *INFN Sezione di Milano;* ^(b) *Dipartimento di Fisica, Università di Milano, Milano, Italy*
- 93 *B.I. Stepanov Institute of Physics, National Academy of Sciences of Belarus, Minsk, Republic of*
Belarus
- 94 *National Scientific and Educational Centre for Particle and High Energy Physics, Minsk, Republic*
of Belarus
- 95 *Department of Physics, Massachusetts Institute of Technology, Cambridge MA, United States of*
America
- 96 *Group of Particle Physics, University of Montreal, Montreal QC, Canada*
- 97 *P.N. Lebedev Institute of Physics, Academy of Sciences, Moscow, Russia*
- 98 *Institute for Theoretical and Experimental Physics (ITEP), Moscow, Russia*
- 99 *National Research Nuclear University MEPhI, Moscow, Russia*
- 100 *D.V. Skobeltsyn Institute of Nuclear Physics, M.V. Lomonosov Moscow State University, Moscow,*
Russia
- 101 *Fakultät für Physik, Ludwig-Maximilians-Universität München, München, Germany*
- 102 *Max-Planck-Institut für Physik (Werner-Heisenberg-Institut), München, Germany*
- 103 *Nagasaki Institute of Applied Science, Nagasaki, Japan*

- 103 Graduate School of Science and Kobayashi-Maskawa Institute, Nagoya University, Nagoya, Japan
- 104 (a) INFN Sezione di Napoli; (b) Dipartimento di Fisica, Università di Napoli, Napoli, Italy
- 105 Department of Physics and Astronomy, University of New Mexico, Albuquerque NM, United States of America
- 106 Institute for Mathematics, Astrophysics and Particle Physics, Radboud University Nijmegen/Nikhef, Nijmegen, Netherlands
- 107 Nikhef National Institute for Subatomic Physics and University of Amsterdam, Amsterdam, Netherlands
- 108 Department of Physics, Northern Illinois University, DeKalb IL, United States of America
- 109 Budker Institute of Nuclear Physics, SB RAS, Novosibirsk, Russia
- 110 Department of Physics, New York University, New York NY, United States of America
- 111 Ohio State University, Columbus OH, United States of America
- 112 Faculty of Science, Okayama University, Okayama, Japan
- 113 Homer L. Dodge Department of Physics and Astronomy, University of Oklahoma, Norman OK, United States of America
- 114 Department of Physics, Oklahoma State University, Stillwater OK, United States of America
- 115 Palacký University, RCPTM, Olomouc, Czech Republic
- 116 Center for High Energy Physics, University of Oregon, Eugene OR, United States of America
- 117 LAL, Université Paris-Sud and CNRS/IN2P3, Orsay, France
- 118 Graduate School of Science, Osaka University, Osaka, Japan
- 119 Department of Physics, University of Oslo, Oslo, Norway
- 120 Department of Physics, Oxford University, Oxford, United Kingdom
- 121 (a) INFN Sezione di Pavia; (b) Dipartimento di Fisica, Università di Pavia, Pavia, Italy
- 122 Department of Physics, University of Pennsylvania, Philadelphia PA, United States of America
- 123 National Research Centre “Kurchatov Institute” B.P.Konstantinov Petersburg Nuclear Physics Institute, St. Petersburg, Russia
- 124 (a) INFN Sezione di Pisa; (b) Dipartimento di Fisica E. Fermi, Università di Pisa, Pisa, Italy
- 125 Department of Physics and Astronomy, University of Pittsburgh, Pittsburgh PA, United States of America
- 126 (a) Laboratório de Instrumentação e Física Experimental de Partículas - LIP, Lisboa; (b) Faculdade de Ciências, Universidade de Lisboa, Lisboa; (c) Department of Physics, University of Coimbra, Coimbra; (d) Centro de Física Nuclear da Universidade de Lisboa, Lisboa; (e) Departamento de Física, Universidade do Minho, Braga; (f) Departamento de Física Teórica y del Cosmos and CAFPE, Universidad de Granada, Granada (Spain); (g) Dep Física and CEFITEC of Faculdade de Ciências e Tecnologia, Universidade Nova de Lisboa, Caparica, Portugal
- 127 Institute of Physics, Academy of Sciences of the Czech Republic, Praha, Czech Republic
- 128 Czech Technical University in Prague, Praha, Czech Republic
- 129 Faculty of Mathematics and Physics, Charles University in Prague, Praha, Czech Republic
- 130 State Research Center Institute for High Energy Physics, Protvino, Russia
- 131 Particle Physics Department, Rutherford Appleton Laboratory, Didcot, United Kingdom
- 132 Ritsumeikan University, Kusatsu, Shiga, Japan
- 133 (a) INFN Sezione di Roma; (b) Dipartimento di Fisica, Sapienza Università di Roma, Roma, Italy
- 134 (a) INFN Sezione di Roma Tor Vergata; (b) Dipartimento di Fisica, Università di Roma Tor Vergata, Roma, Italy
- 135 (a) INFN Sezione di Roma Tre; (b) Dipartimento di Matematica e Fisica, Università Roma Tre, Roma, Italy
- 136 (a) Faculté des Sciences Ain Chock, Réseau Universitaire de Physique des Hautes Energies - Université Hassan II, Casablanca; (b) Centre National de l’Energie des Sciences Techniques Nucleaires, Rabat; (c) Faculté des Sciences Semlalia, Université Cadi Ayyad, LPHEA-Marrakech; (d) Faculté des Sciences, Université Mohamed Premier and LPTPM, Oujda; (e) Faculté des sciences, Université Mohammed V-Agdal, Rabat, Morocco
- 137 DSM/IRFU (Institut de Recherches sur les Lois Fondamentales de l’Univers), CEA Saclay

- (Commissariat à l’Energie Atomique et aux Energies Alternatives), Gif-sur-Yvette, France
- 138 Santa Cruz Institute for Particle Physics, University of California Santa Cruz, Santa Cruz CA, United States of America
- 139 Department of Physics, University of Washington, Seattle WA, United States of America
- 140 Department of Physics and Astronomy, University of Sheffield, Sheffield, United Kingdom
- 141 Department of Physics, Shinshu University, Nagano, Japan
- 142 Fachbereich Physik, Universität Siegen, Siegen, Germany
- 143 Department of Physics, Simon Fraser University, Burnaby BC, Canada
- 144 SLAC National Accelerator Laboratory, Stanford CA, United States of America
- 145 ^(a) Faculty of Mathematics, Physics & Informatics, Comenius University, Bratislava; ^(b) Department of Subnuclear Physics, Institute of Experimental Physics of the Slovak Academy of Sciences, Kosice, Slovak Republic
- 146 ^(a) Department of Physics, University of Cape Town, Cape Town; ^(b) Department of Physics, University of Johannesburg, Johannesburg; ^(c) School of Physics, University of the Witwatersrand, Johannesburg, South Africa
- 147 ^(a) Department of Physics, Stockholm University; ^(b) The Oskar Klein Centre, Stockholm, Sweden
- 148 Physics Department, Royal Institute of Technology, Stockholm, Sweden
- 149 Departments of Physics & Astronomy and Chemistry, Stony Brook University, Stony Brook NY, United States of America
- 150 Department of Physics and Astronomy, University of Sussex, Brighton, United Kingdom
- 151 School of Physics, University of Sydney, Sydney, Australia
- 152 Institute of Physics, Academia Sinica, Taipei, Taiwan
- 153 Department of Physics, Technion: Israel Institute of Technology, Haifa, Israel
- 154 Raymond and Beverly Sackler School of Physics and Astronomy, Tel Aviv University, Tel Aviv, Israel
- 155 Department of Physics, Aristotle University of Thessaloniki, Thessaloniki, Greece
- 156 International Center for Elementary Particle Physics and Department of Physics, The University of Tokyo, Tokyo, Japan
- 157 Graduate School of Science and Technology, Tokyo Metropolitan University, Tokyo, Japan
- 158 Department of Physics, Tokyo Institute of Technology, Tokyo, Japan
- 159 Department of Physics, University of Toronto, Toronto ON, Canada
- 160 ^(a) TRIUMF, Vancouver BC; ^(b) Department of Physics and Astronomy, York University, Toronto ON, Canada
- 161 Faculty of Pure and Applied Sciences, University of Tsukuba, Tsukuba, Japan
- 162 Department of Physics and Astronomy, Tufts University, Medford MA, United States of America
- 163 Centro de Investigaciones, Universidad Antonio Narino, Bogota, Colombia
- 164 Department of Physics and Astronomy, University of California Irvine, Irvine CA, United States of America
- 165 ^(a) INFN Gruppo Collegato di Udine, Sezione di Trieste, Udine; ^(b) ICTP, Trieste; ^(c) Dipartimento di Chimica, Fisica e Ambiente, Università di Udine, Udine, Italy
- 166 Department of Physics, University of Illinois, Urbana IL, United States of America
- 167 Department of Physics and Astronomy, University of Uppsala, Uppsala, Sweden
- 168 Instituto de Física Corpuscular (IFIC) and Departamento de Física Atómica, Molecular y Nuclear and Departamento de Ingeniería Electrónica and Instituto de Microelectrónica de Barcelona (IMB-CNM), University of Valencia and CSIC, Valencia, Spain
- 169 Department of Physics, University of British Columbia, Vancouver BC, Canada
- 170 Department of Physics and Astronomy, University of Victoria, Victoria BC, Canada
- 171 Department of Physics, University of Warwick, Coventry, United Kingdom
- 172 Waseda University, Tokyo, Japan
- 173 Department of Particle Physics, The Weizmann Institute of Science, Rehovot, Israel
- 174 Department of Physics, University of Wisconsin, Madison WI, United States of America
- 175 Fakultät für Physik und Astronomie, Julius-Maximilians-Universität, Würzburg, Germany

- 176 *Fachbereich C Physik, Bergische Universität Wuppertal, Wuppertal, Germany*
- 177 *Department of Physics, Yale University, New Haven CT, United States of America*
- 178 *Yerevan Physics Institute, Yerevan, Armenia*
- 179 *Centre de Calcul de l'Institut National de Physique Nucléaire et de Physique des Particules (IN2P3), Villeurbanne, France*
- ^a *Also at Department of Physics, King's College London, London, United Kingdom*
- ^b *Also at Institute of Physics, Azerbaijan Academy of Sciences, Baku, Azerbaijan*
- ^c *Also at Novosibirsk State University, Novosibirsk, Russia*
- ^d *Also at TRIUMF, Vancouver BC, Canada*
- ^e *Also at Department of Physics, California State University, Fresno CA, United States of America*
- ^f *Also at Department of Physics, University of Fribourg, Fribourg, Switzerland*
- ^g *Also at Departamento de Física e Astronomia, Faculdade de Ciências, Universidade do Porto, Portugal*
- ^h *Also at Tomsk State University, Tomsk, Russia*
- ⁱ *Also at CPPM, Aix-Marseille Université and CNRS/IN2P3, Marseille, France*
- ^j *Also at Università di Napoli Parthenope, Napoli, Italy*
- ^k *Also at Institute of Particle Physics (IPP), Canada*
- ^l *Also at Particle Physics Department, Rutherford Appleton Laboratory, Didcot, United Kingdom*
- ^m *Also at Department of Physics, St. Petersburg State Polytechnical University, St. Petersburg, Russia*
- ⁿ *Also at Louisiana Tech University, Ruston LA, United States of America*
- ^o *Also at Institutio Catalana de Recerca i Estudis Avancats, ICREA, Barcelona, Spain*
- ^p *Also at Department of Physics, National Tsing Hua University, Taiwan*
- ^q *Also at Department of Physics, The University of Texas at Austin, Austin TX, United States of America*
- ^r *Also at Institute of Theoretical Physics, Ilia State University, Tbilisi, Georgia*
- ^s *Also at CERN, Geneva, Switzerland*
- ^t *Also at Georgian Technical University (GTU), Tbilisi, Georgia*
- ^u *Also at O Chadai Academic Production, Ochanomizu University, Tokyo, Japan*
- ^v *Also at Manhattan College, New York NY, United States of America*
- ^w *Also at Institute of Physics, Academia Sinica, Taipei, Taiwan*
- ^x *Also at LAL, Université Paris-Sud and CNRS/IN2P3, Orsay, France*
- ^y *Also at Academia Sinica Grid Computing, Institute of Physics, Academia Sinica, Taipei, Taiwan*
- ^z *Also at School of Physics, Shandong University, Shandong, China*
- ^{aa} *Also at Moscow Institute of Physics and Technology State University, Dolgoprudny, Russia*
- ^{ab} *Also at section de Physique, Université de Genève, Geneva, Switzerland*
- ^{ac} *Also at International School for Advanced Studies (SISSA), Trieste, Italy*
- ^{ad} *Also at Department of Physics and Astronomy, University of South Carolina, Columbia SC, United States of America*
- ^{ae} *Also at School of Physics and Engineering, Sun Yat-sen University, Guangzhou, China*
- ^{af} *Also at Faculty of Physics, M.V.Lomonosov Moscow State University, Moscow, Russia*
- ^{ag} *Also at National Research Nuclear University MEPhI, Moscow, Russia*
- ^{ah} *Also at Department of Physics, Stanford University, Stanford CA, United States of America*
- ^{ai} *Also at Institute for Particle and Nuclear Physics, Wigner Research Centre for Physics, Budapest, Hungary*
- ^{aj} *Also at Department of Physics, Oxford University, Oxford, United Kingdom*
- ^{ak} *Also at Department of Physics, The University of Michigan, Ann Arbor MI, United States of America*
- ^{al} *Also at Discipline of Physics, University of KwaZulu-Natal, Durban, South Africa*
- ^{am} *Also at University of Malaya, Department of Physics, Kuala Lumpur, Malaysia*
- * *Deceased*